RNI: DELENG/2005/15153
Publication: 15th of every month
Posting: 19th/20th of every month at NDPSO

No: DL(E)-01/5079/11-13
Licensed to post without pre-payment U(E) 28/2011-13
Rs.100

ISSN 0973-2136

www.mycoordinates.org

Coordinates

Volume IX, Issue 8, August 2013

THE MONTHLY MAGAZINE ON POSITIONING, NAVIGATION AND BEYOND

analysis by 3-D affine deformations

Navigation • GIS • Cadastral

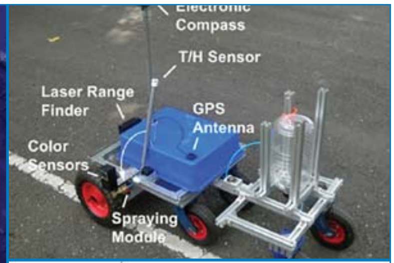

In this issue

Coordinates Volume 9, Issue 8, August 2013

Articles

Columns

This issue has been made possible by the support and good wishes of the following individuals and companies
Adnan AL-Jaber, Anoop Nautiyal, Bo-Han Wu, Carla Wheeler, Chung-Liang Chang, James L Farrell, Kang, Sang-Gu , Kim, Kyung-Il, Kim, Tae-Hoon, and Yong-Cheng Huang and; Ashtech, CHC, Effigis, Foif, Hemisphere GPS, HiTarget, Javad, MicroSurvey, Pentax, Navcom, NovAtel, Sensonor, South, Techequip, Trimble, and many others.

Mailing Address
A 002, Mansara Apartments
C 9, Vasundhara Enclave
Delhi 110 096, India.
Phones +91 11 22632607, 98102 33422, 98107 24567
Fax +91 11 22632607

Email
[information] talktous@mycoordinates.org
[editorial] bal@mycoordinates.org
[advertising] sam@mycoordinates.org
[subscriptions] iwant@mycoordinates.org

Web www.mycoordinates.org

Annual subscription (12 issues) [India] Rs.1,200 [Overseas] US$80

Printed and published by Sanjay Malaviya on behalf of Centre for Geoinformation Technologies at A221 Mangal Apartments, Vasundhara Enclave, Delhi 110096, India.

Editor Bal Krishna

Owner Centre for Geoinformation Technologies

Designed at Spring Design (springdesign@live.com)

Printer Thomson Press India Ltd., B 315, Okhla Phase I, New Delhi - 110020, India

This issue of Coordinates is of 64 pages, including cover.

X91^{+} GNSS - The industry's performance and reliability standard

- ***TRACKING EVERY SIGNAL AND EVERY SATELLITE***
  Advanced 220-channel GNSS technology for state-of-the-art RTK accuracy and reliability
- ***FLEXIBLE AND SCALABLE***
  Internal UHF and Cellular data modems; bundled with Carlson SurvCE or CHC Landstar field software
- ***EFFICIENT***
  Small, lightweight and rugged design for the most demanding field work
- ***SUPPORT***
  Worldwide network of local service centers and dealers

India on a high

Finally, it happened on July 2, 2013.

India successfully launched IRNSS-1A

The first satellite of Indian Regional Navigation Satellite System (IRNSS),

Of the seven satellites constellation planned.

Recent reports suggest that all is well.

The Navigation and Ranging Payload In Orbit Tests (IOT) are completed.

And all operations are normal.

The entire constellation is expected to be completed by 2015-16.

This launch definitely enthuse the confidence.

That this ambitious infrastructure project will continue to progress,

And that too as per the schedule.

Bal Krishna, Editor
bal@mycoordinates.org

TECH EQUIP ENTERPRISES

GAGAN DGPS SBAS RECEIVERS SINCE 2007
UNCHALLANGED POSITIONING ACCURACY (<2M) NOW AFFORDABLE FOR SCIENTIFIC COMMUNITY

EXPERIENCE DGPS ACCURACY WITHOUT EXPENSIVE BASE AND ROVER POST PROCESSING CONFIGURATIONS
USE ISRO'S GAGAN SBAS DGPS SIGNAL TO GET
<1M ACCURACY PREMIUM RANGE **<2M ACCURACY STANDARD RANGE**

PREMIUM RANGE : - GAGAN SBAS +PPP Carrier phase measurement

WORLD'S FIRST & MOST ACCURATE GAGAN SBAS +PPP, IP 67 - PDA GPS

GAGAN +PPP

- Windows Mobile 6.5
- RAM / ROM - 512MB / 512MB
- Display 4.3", High brigtness 480x800 LED display
- 5 megapixel digital camera
- Battery 3.7V 5000mAh Li-Poly rechargeable battery
- WLAN Support 802.11 2.4GHz b/g/n mode
- Bluetooth 2.1+EDR (No audio profile)
- USB OTG
- 3G Optional
- Embedded with Micro SD card slot
- Designed for IP67 Dust & Water Protection
- Compliant with MIL-STD 810F Standard

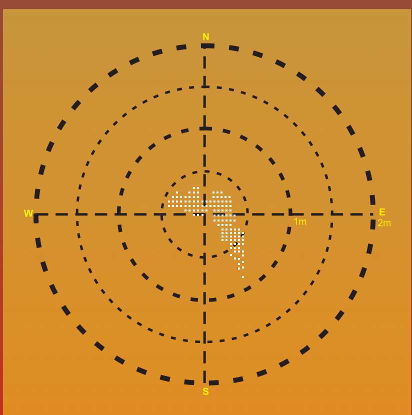

WORLDS MOST PRECISE SBAS DATA COLLECTOR WITH <1M ACCURACY WITHOUT POST PROCESSING WITHOUT A BASE STATION

PARISHUD

Precise GAGAN Positioning
(SBAS+CARRIER PHASE MEASUREMENT)

+

SuperPad 3

a full-function mobile GIS application

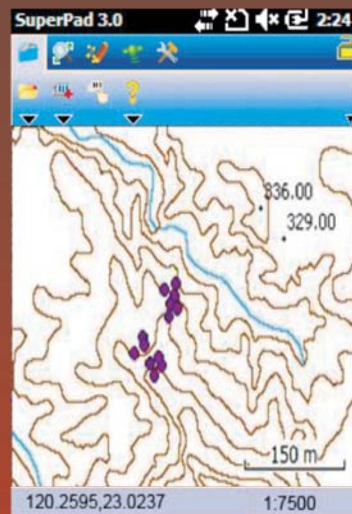

Both together at just

= **₹. 60,000/-***

COST PERFORMANCE RATIO FAR AHEAD

STANDARD RANGE : - GAGAN

INDRA DHANUSH
USB MINIATURE
2m 2DMRS
₹. 5000/- *

SX BLUE
IP-67 BATTERY BUILT-IN
1m 2DMRS
₹. 1,00,000/- *

DHARTI
IP-54 GIS DATA LOGGER
1.5m 2DMRS
₹. 32,000/- *

TECH EQUIP ENTERPRISES

(SPEAR HEADING GAGAN BASED SOLUTIONS)

388, Street No. 8, East Marredpalli, Secunderabad - 500 026. (A.P.)
Contact : R. Mohan 9885975365, Email : techequipenterprises@yahoo.com

* - Approximate Price

Earthquake analysis by 3-D affine deformations

Changes in coordinates at stations affected by earthquakes have been monitored successfully, for years, with precision using satellite navigation. Results of interest have then been produced in the past through processing the outcome by conventional means. Those methods can now be augmented by applying entirely different criteria: deformation states associated with affine transformations.

James L Farrell
VIGIL Inc., Institute of Navigation Pacific PNT 2013, Honolulu Hawaii, USA

In this first application of morphometrics to earthquakes, plot sequences are first provided for coordinate shifts, rotations, and uniform scaling on each separate day. In addition to those seven time histories from Procrustes representations, five more offer further insight: shape states (three shear and two nonuniform scaling). For those, classical (two-dimensional; '2-D') methods from anatomy had to be extended to 3-D. All were obtained for landmark coordinate sets reported daily for four weeks before and after the 2011 Tohoku quake. Findings exhibit encouraging prospects for anticipation, in time and spatially. Data provided herein enables readers to verify sample results.

Introduction

An illustration of the methodology used here is available from selected station location histories before and after the Tohoku quake in 2011. Figure 1 shows the chosen stations on a map [1] and Figure 2 depicts them following rotations and normalizations to be described herein. The eleven stations are represented as a 3-D structure consisting of point masses all tethered to their collective centroid by weightless connecting arms that are not quite rigid. With migration the centroid shifts accordingly while the connecting arms rotate and deform to accommodate as necessary. Migration irregularities preclude exact mathematical characterization for the pattern of accommodating adjustments, but a daily affine transformation sequence serves as a useful model for analysis and interpretation - with prospects for anticipating earthquakes in the future.

Background from related fields

Methods from branches of multiple disciplines are highly relevant. For this

Figure 1: Selected observation stations

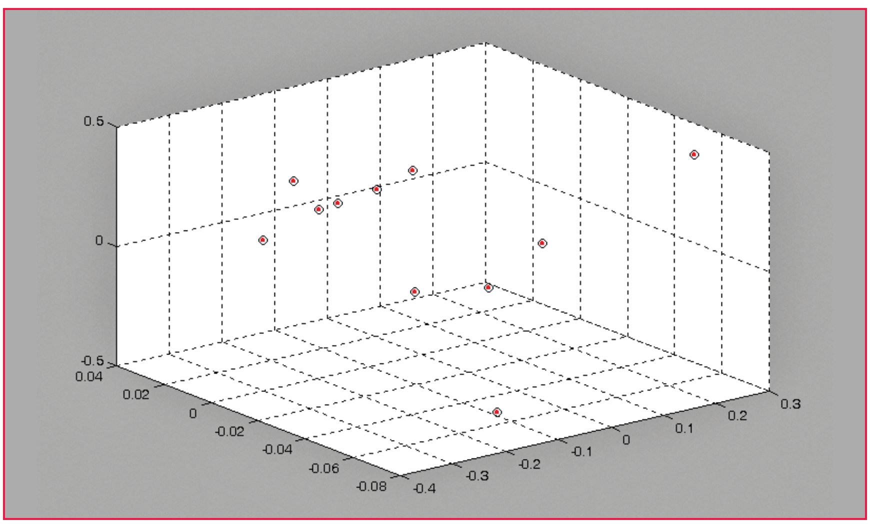

Figure 2: Transformed and rescaled point mass array

first 3-D affine deformation analysis applied to earthquakes, presentation calls for recognition of pertinent sources. At the same time, their descriptions here cannot exceed length restrictions. A full mathematical development, accompanied by the complete set of results to be shown, would violate length limitations. Alternatively that development, without the results, could cause readers to feel "lost in a sea of equations" with any potential benefits yet to be seen. Complex equations are therefore absent from this paper; methods are described verbally in reasonable detail but, for derivations, heavy reliance is placed on selected references. For ease of familiarization, applicable reference material is focused as narrowly as permissible. Wherever possible, verbal descriptions are worded so that the reference will not be needed by those familiar with material being discussed.

Mathematics

Developments of standard tools itemized in this subsection, including derivations, are available from many sources. Major operations include 1) minimum variance estimation, 2) coordinate rotations, 3) diagonalization of 3×3 square matrices, 4) singular value decomposition (svd) of rectangular matrices, and 5) 4×4 affine transformations.

Coverage of the first three items, with some subtle features needed for this specific application included, can be found in [2]. With usage of the block (rather than sequential) estimation, the brief development on pages 159-162 suffices. Even that is more general than needed for the steps followed here (though not for recommended future extensions). Pages 36-38 of [2] cover 3-D coordinate rotations, but that latter page shows a popular small-angle representation acceptable in most operations – though not used here. When rotating vectors of enormous size (hundreds of km), adequate precision must be ensured. Here that translates into approximating the cosine of a small angle – not by unity but by a two-term representation. A direction cosine matrix that rotates through a small angle θ about any axis with unit column vector **E**, contains three ingredients:

- a 3×3 identity matrix multiplied by $(1 - ½\theta^2)$
- θ multiplied by a skew-symmetric matrix corresponding to vector cross product operator (**E** ×)
- $½\theta^2$× (outer product **E** postmultiplied by its transpose) Those unfamiliar can examine Eq. (2-48) of [2], not limited to small angles.

Another transformation involves reexpression of latitude/longitude/altitude into earth-centered, earth-fixed (ECEF) coordinates. Again the operation is standard; those unfamiliar can examine Eq. (7-31), with (3-18, -19, -22), of [2]. Also the inverse is described in addendum 5.E of [3]. Diagonalization of a square matrix is defined in [2] by Eqs. (II-20, -21, -22), with examples given in pages following them. Standard algorithms are common, e.g.,

[evec, eval] = eig(matrix)

in MATLAB. For matrices that are rectangular rather than square a related operation (svd) is used: adequate for purposes here, again from MATLAB,

$[\mathbf{M_U}, \mathbf{D}, \mathbf{M_V}] = \text{svd}\ (\mathbf{U}\ \mathbf{V^T})$

The role of the eigenvector matrix denoted "evec" plus the factors denoted $\mathbf{M_U}$, $\mathbf{M_V}$, **U**, and the transpose $\mathbf{V^T}$ of **V**, are defined in subsections that follow.

Affine transformations, central to this investigation, offer a much wider scope of effects including translation, scaling, and deformation as well as rotation. The standard 4×4 affine transformation in 3-D, being homogeneous, has one less independent state than the number (sixteen) of matrix elements. The fifteen independent states can be categorized in five sets of three, each set having *x*-, *y*-, and *z*-components for translation, rotation, perspective, scaling, and shear. Immediately the three degrees-of-freedom associated with perspective are irrelevant for purposes here. In addition both translation and rotation, clearly having no effect on shape, can be analyzed separately – and the same is likewise true of uniform scaling. It is thus widely known that there are five "shape states" involved in 3-D affine deformations, three for shear and two for nonuniform scaling.

One way to describe shape states is to note their effects in 2-D, where there is only one for nonuniform scaling (which deforms a square into a rectangle) and one for shear (which deforms a rectangle into a parallelogram). Therefore it is suggested here that added insight into earthquake investigation can be obtained by analyzing affine features – with specific attention given to their individual traits (degrees-of-freedom).

For those unfamiliar with affine matrixes, [4] provides an excellent thorough introduction plus numerous examples. Due to their central role, they will appear repeatedly in multiple discussions to follow.

Anatomy

Familiarization with the topic now to be broached sometimes begins with the example of facial features (e.g., tip of chin, corners of the eyes and mouth). Those qualified, however, identify landmarks on other anatomical structures for further study (e.g., as a possible diagnostic tool if certain deformations correlate with some affliction). When measurements (e.g., from x-ray images) are processed as described shortly, specific landmarks – even from a wide variety of patients (any nationality, any race, all ages, both sexes) – are found to cluster with some degree of consistency. That trait is physiological, not an artifact of the processing. Also, when the landmarks are remapped after extraction of affine deformations, the clusters shrink; theoretically if *only* affine deformations were present, clusters would converge to discrete points.

The universally recognized reference [5] contains thorough descriptions of the entire process plus a wealth of results, along with a full derivation (from pages 138-142) developed by the author of [6] for affine deformation states – all in 2-D. Needless to say this presentation will not include that derivation, let alone its 3-D extension. What can be realistically offered here will nevertheless enable partial application of this methodology to other data sets, with or without this author's involvement. Not all of the results to follow require the complete deformation analysis. In generating those results, some very revealing features arose in earlier portions of the overall procedure – without requiring full pursuit to final determination of 3-D deformations. For this data set, at least, understanding can thus be brought to a significant level with just the *Procrustes* representation, described succinctly as follows:

The previously defined structure of K point masses and nonrigid connecting arms ($K = 11$ in this study) is first transformed into principal axes of inertia (next subsection) and the origin is translated to the centroid. Division by the root sum square of all coordinates then produces an array containing $3K$ dimensionless positive and negative numbers whose sum of squares is unity.

With normalization of all magnitudes an orthogonal matrix, computed for each separate day of the sequence, minimizes that day's sum of squares of rotated landmark changes from the first ("Day #**I**"). It is formed, as on page 98 of [6] but with notation modified here, as a product $\mathbf{M_V}\,\mathbf{M_U}^{\mathbf{T}}$ of outer factors from svd with **U** and **V**, $3 \times K$ matrices produced by the set of Procrustes operations just defined, acting on the data from Day #**I** and each subsequent day, respectively.

After forming all Procrustes coordinate matrices and storing columns of **U** into vector **U**, affine transformation provides an array **u** of small adjustments for each day's fitted array **V**, nominally characterized as **U+u**. Explanation is now in order, due to differences from applications to anatomy. Here there is no need to form an average mesh; Day #**I**'s coordinate set serves as the comparison reference throughout. Also the coordinate adjustments, shape states, and rotations from svd here are are not merely small; they are minuscule – of order 1.e-8. Still the need for precision calls for rigorous computations; over a span of 1000 km, $0.01\ \mu$radian rotations generate cm displacements. Even with **u** orthogonal to **U** an adjustment is made; **u** is summed – not with **U** but with **U**/ |**U+u** | – see next subsection.

Also of potential interest from the field of anatomy are further deformations represented by a thin plate spline (TPS, which minimizes approximate squared curvature integrated over a surface defined by a landmark set). Nonlinear (unlike affine) deformations are applicable over only local regions rather than entire structures. Full implications of that issue, quite broad in physiological studies, involve complex topics not needed for this landmark analysis (e.g., sophisticated mathematics of Riemannn manifolds and the impact on detailed algorithms for *dense correspondence* in positioning pixels between landmarks of high resolution images). For this application only the TPS is considered – and only briefly, at that – since results obtained show that variations in the day-to-day bending energy obtained from it are negligible for practical purposes.

Mechanics

Only a few concepts from this branch were used here. It was foreshadowed earlier that adding a miniscule vector orthogonal to a unit vector must not result in a significant length increase. That "arc length constraint" is modified somewhat here; more generally, although the affine deformation vector **u** can include expansion/contraction effects, no *artificial* elongation is introduced through vector addition (hence division of **U** by |**U+u** |). Although that same principle theoretically applies to the TPS (which equates curvature to a second derivative without the slight shortening just described), that adjustment has not been found necessary (nor feasible) for TPS fitting.

One of the earliest steps taken prior to determination of deformations is formation of the inertia matrix for the reference configuration (in this case, the set of K point mass landmarks in 3-D on Day #**I**). With those ECEF coordinates in a $3 \times K$ array **U** and its $K \times 3$ transpose $\mathbf{U^T}$ along with its $3K \times 1$ vector **U**, the inertia matrix contains two terms,

- the product $\mathbf{U^T U}$ multiplied by the 3×3 identity matrix
- the product $\mathbf{UU^T}$ multiplied by -1.

Their sum is the matrix to be diagonalized, described earlier.

Strength of Materials

Deformations have spatial derivatives in along-axis and across-axis directions. The latter, in order, are associated with slopes, components of curvature (proportional to bending moments), and curvature gradients (proportional to shearing stress) while along-axis deformations (extension and contraction) are related to tensile and compressive stress. In-depth pursuit of these and other additional forces (e.g., friction) would clearly involve still another field of endeavor, i.e., geology, to take into account tectonic plate characteristics (composition, inhomogeneity, irregular cross-section geometry, elasticity, etc.). Although beyond scope here, a limited effort toward that direction was originally intended, by using an available TPS program. The program did quantify bending energy but, at least for the period of primary interest (pre-quake), those temporary elastic deformations lowered that priority for the data studied. Reasons are traceable to the diminutive

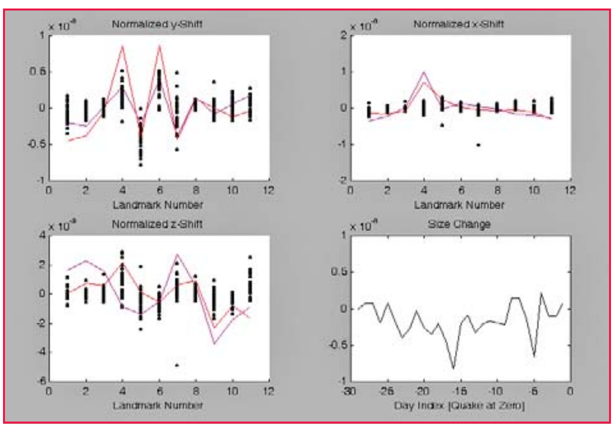

Figure 3 : Changes from comparison reference ("Day #I"), in principal axes and relative scaling, pre-quake

changes in coordinates compared to the distances spanned. Dominance of other factors would not justify further emphasis on nonlinear deformations.

Procedure

A synopsis of steps summarizes the preceding descriptions:

- select an ensemble of station histories to be analyzed
- acquire data in most reliable and accurate form
- assemble coordinate data into arrays to prepare operations
- use each separate day's landmark set centroid as origin
- form the inertia matrix of the first day's landmark set
- diagonalize the inertia matrix for principal axis resolution
- form a direction cosine matrix from the eigenvectors
- shrink each day's centered landmark coordinate sum of squares to unity (this step could either precede or follow the next)
- transform each day's landmark data set through the 3×3 orthogonal matrix
- rotate again per svd from each day's data *vs* Day #**I**
- compute estimates for each day's five shape states
- apply shape states to the reference (Day #**I**) data
- backtrace steps to reconstruct input data; evaluate the fit based on residuals
- prepare all results for dissemination/presentation

Completion of all steps can enable interpretation and evaluation of outcome as means for quake prediction. Toward that objective, recommendations for further tasks to be pursued follow the results now to be presented.

Quantitative results

Disturbances appearing in advance are seen from plots using an abscissa indexed with the quake at zero. From data files starting 29 days prior, then, "Day #**I**" is indexed at -29.

Each x, y, and z landmark migration in Figure 3 appears as a single dot, except for those depicted by two solid lines used to show some deviations from general patterns. Occurring five days and sixteen days before the quake, they are somewhat more pronounced in the lower right plot. Further changes after the quake are of course larger, but higher priority is attached here to pre-quake behavior.

While early disturbances are entirely consistent with past experience, processing the data in another way can lend further insight. Here the changes are reexpressed in terms of the deformed Procrustes representation used for this study. To begin that portrayal, pre- plus post-quake centroid shifts and pre-quake small rotational adjustments are shown in Figure 4 and 5, respectively.

The permanence of change in Figure 4 is obvious and not at all surprising. Again the foreshadowing at 5 and 16 days pre-quake are detectable, and of course would be more clearly visible on a half-duration plot (i.e., terminating one day before the quake, as Figure 5 does for the rotational history). The last two plots offer some added premonitions. The temporary character of these advance disturbances (tendency to return toward earlier forms) is suggestive of elastic deformations, but

- only a partial restoration occurs, and
- there is some growth of deformation peaks.

Issues just noted are revisited in later sections. First it is of interest to follow through with additional behavior patterns, starting with a serendipitous clue that arose while validating the small-angle rotations of Figure 5.

Formation of the orthogonal matrix with the outer factors from the svd, as previously described, was first shown to provide the minimization as promised. That verification produced Figure 6, now described as follows: Separately in sequence, centroids of each day's K landmark appendages colocate with that of Day #**I**. Migration nonuniformity precludes coincidence of point mass extremities but the sum of squared separation distances is minimized by the orthogonal matrix from the svd. Multiplying the angle through a span of values (from too little to too much rotation) always made the closest combination for a multiplier of unity. Generally the sum of squares tends to grow as the quake draws near (***except*** for the same days already noted and also one day ahead. No definitive diagnosis will be attempted from this amount of data, except to say that the phenomenon warrants wider investigation.

As one step toward wider scrutiny, sensitivity to the rotation axis direction was also determined. Resulting 3-D

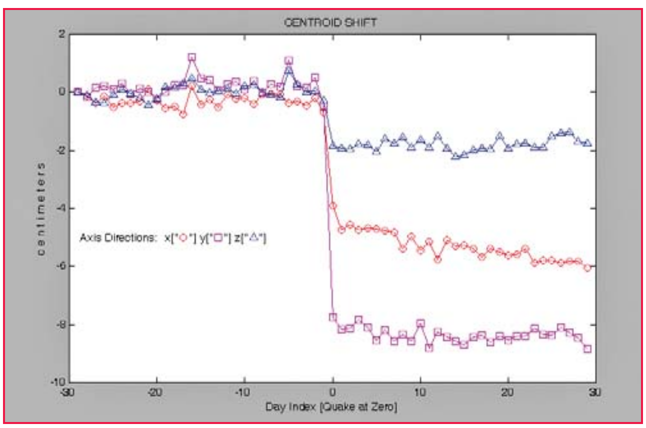

Figure 4: Centroid movement, before and after quake

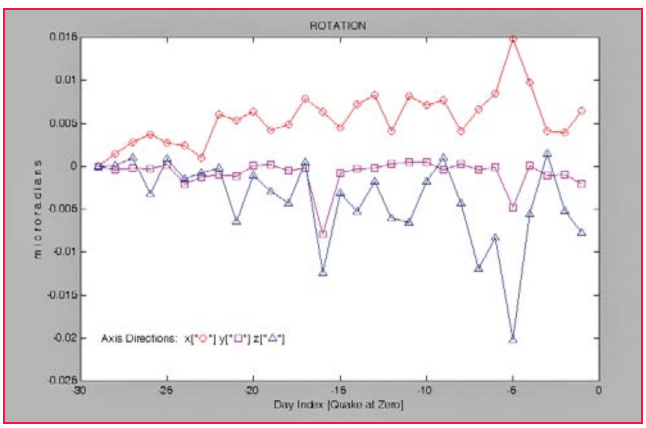

Figure 5: Rotation for Procrustes fit, pre-quake

Photo: Sindre Lundvold

NORWEGIAN EXTREME ARTIST, ESKIL RONNINGSBAKKEN, ON A UNICYCLE AT TROLLVEGGEN, THE TALLEST VERTICAL ROCK FACE IN EUROPE. NORWAY, 2010.

AMAZING SKILLS OF THE WORLD

INSPIRE US ...

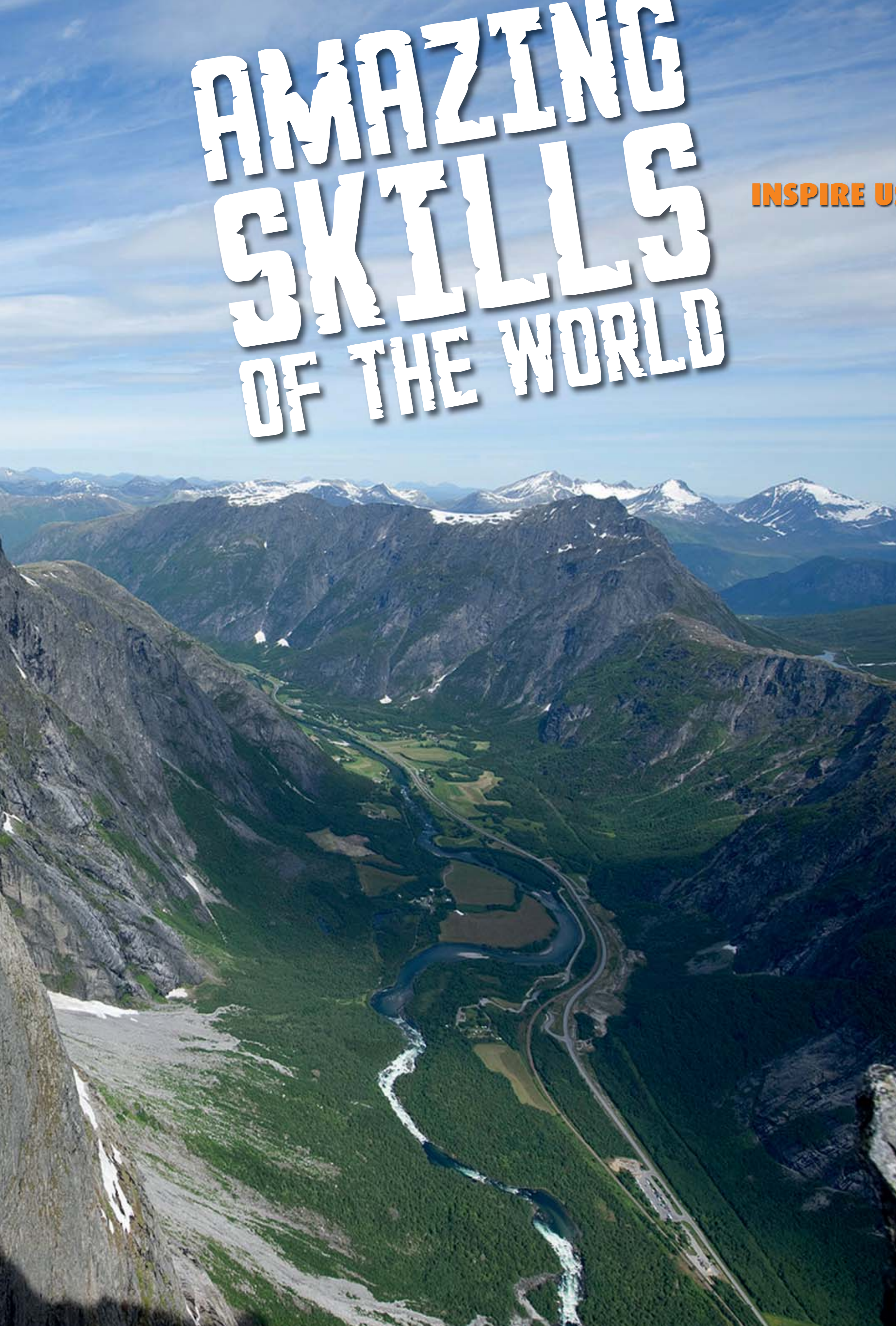

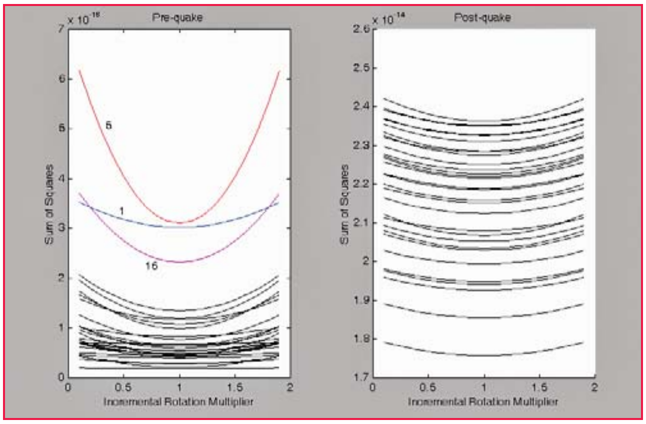

Figure 6: Rotation sensitivity, before and after quake

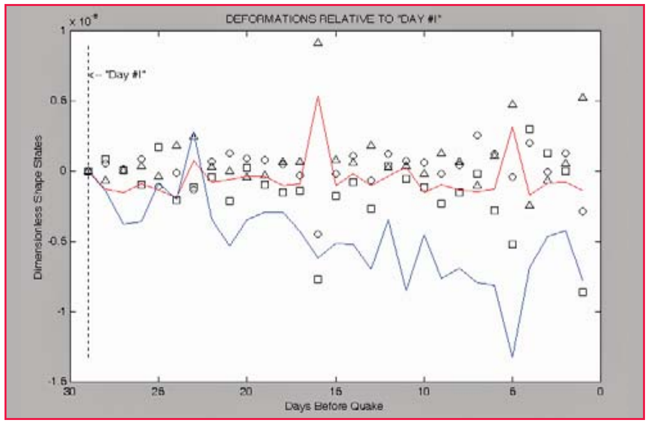

Figure 7: Deformation states, pre-quake

images for 29 days cannot be plotted together without masking each other, but the outcome is similar. The three days noted in Fig. 6 exhibited abnormal sensitivity to the direction, as well as the amount, of rotation. Furthermore, also on those same days, at least three shape states (not always the exact same set) temporarily jumped beyond their normally moderate growth trend.

Before switching attention to the shape states, it is noted that behavior of this data set is not guaranteed to hold in general. Other attributes could arise from chosen landmark sets with dissimilar layout geometries (or even from an alternative choice of shape states for this data set – recall that there are two expansion / contraction states covering three directions). These points facilitate understanding Figure 7 but, again, no generalization will be attempted here; data from other quakes could show different behavior.

Figure 7 is seen to be consistent with discussion preceding it, while exhibiting numerical values comparable to the rotation states of Figure 5. Also, local pre-quake peaks are again apparent in the expansion / contraction state line plots and the symbols representing shear states. Immediately a question can arise, regarding conformance of this model to migrations actually observed. Numerous plots *vs* time and *vs* landmark number, made to evaluate that conformance, are discussed next.

Coordinate plots computed from the model, together with actual observations, *seem* impressive but not informative (points "coincide" when migrations are dwarfed by distances between landmarks). Alternatively a migrations-only plot, showing departures of modeled from observed values, exhibit the limitations more clearly - but without indicating what constitutes "good" performance. Figure 8 exemplifies the information desired by showing migrations actually observed together with errors in modeling them.

The total volume of data (in three directions from eleven landmarks over a period of weeks) necessitated a way to compact the results for this affine model. That effort, applied to RSS values (3-D x, y, z), produced Figure 9 described as follows: Most residuals (shown with a dot •) fall very near or below the dashed horizontal line at *2* cm. Exceptions are

- values obtained at 16 and 5 days pre-quake (the main "early warning" days, light dashed vertical lines)
- landmark #5 (closest to the epicenter), whose residuals are enclosed within a square
- two others (shown encircled) at about *2.2* and *2.6* cm.

To reiterate, all residuals are below *4* cm., almost 98% are below *3*, and over 91% are below *2*. All but two of the values significantly above *2* cm are either from the station nearest epicenter or from one of the key early warning days.

With 3-D RSS migration reaching a maximum of almost *15* cm amidst dispersions of a few cm, these results are consistent with performance expected from minimum variance estimation. By analogy with a straight line or low order curve fitted to scattered empirical data, a least squares fit here captures the larger migrations while accepting residuals commensurate with the dispersion in the data.

Some further discussion of these residuals is warranted. The plot of this full set in Figure 9 was preceded by a partial glimpse (Figure 8), in one of three principal (not ECEF) axes from one of eleven landmarks. Few partial plots look as good as that sample. For landmarks with smaller migrations (*4* or *5* cm maximum), a nominal *2*-cm dispersion is less impressive – and individual excursion components from some landmarks were in fact less than *2* cm. What those cases contribute, to be blunt, "just looks like a bunch of dots thrown all over the place." A fitted model *will not* adhere to the points. Attempts to force model fidelity are readily dismissed; many will recall MATLAB's "doomsday" polynomial fitted to empirical global population history.

Model credence for data analyzed here rests on acceptance of *2*-cm residuals as a reasonable (though admittedly not trivial) price to pay for a means of characterization. Immediately a caveat might be raised: Shouldn't that be changed – contingent on acceptance of *4*-cm residuals? Actually no; aside from the two circled points in figure 9 (beyond *2* cm by modest amounts), the "problem" of larger residuals is in reality the *opposite* of a problem. They offer valuable revelations, in time (premonitions at 16 and 5 days pre-quake) and spatially – most of them correspond to the landmark closest to epicenter! As with other facets of this investigation, no generalization will be attempted – but other quakes should be examined for these traits.

Data for verification

As promised, data will now be included to enable duplication of certain results – and subsequent application to observations from other quakes. A full data set, even from the limited scope of this study, would be unwieldy – but coordinates at Day #**I** and at five days prequake allow revealing traits to be exhibited. Those values, in centimeters, are obtained through multiplication by *1.e+8* the next two tabulations for x, y, and z:

Day #I

-3.53018564421	4.11879729786	3.34403687240
-2.67442738639	3.75714316626	4.39152161522
-2.99526661754	2.99044454616	4.75557583584
-3.18629373399	5.28662428008	1.60115832181
-3.99752536845	3.27687093992	3.72421844777
-3.58082845246	1.39969815294	5.07218511128
-3.85526304091	3.42743255339	3.74102026120
-3.46532105841	2.63826932806	4.64408536835
-5.22718788718	2.55188072282	2.60761806619
-4.49060536141	3.48389481290	2.88492824099
-5.07131269039	3.56836358429	1.48890436247

5 Days Pre-Quake

-3.53018564968	4.11879729911	3.34403688006
-2.67442739059	3.75714316466	4.39152162098
-2.99526661834	2.99044454302	4.75557583842
-3.18629376801	5.28662440323	1.60115838489
-3.99752534888	3.27687093953	3.72421844403
-3.58082845686	1.39969815729	5.07218511662
-3.85526303470	3.42743254589	3.74102025522
-3.46532106200	2.63826932401	4.64408536602
-5.22718787822	2.55188071656	2.60761806226
-4.49060536767	3.48389481451	2.88492824690
-5.07131270561	3.56836359610	1.48890436839

The following results are verifiable from Day #**I** data:

The inertia matrix is *1.e+17* *

2.4754	-0.1670	-0.5725
-0.1670	2.1793	0.7581
-0.5725	0.7581	1.6339

with eigenvalues *1.e+17* *

[2.1885 3.1018 0.9983]

and eigenvectors producing the matrix "evec"

0.7239	-0.6369	-0.2651
0.6693	0.5550	0.4940
0.1675	0.5351	-0.8280

From both days' centroid-referenced coordinates the svd produces a small-angle rotation vector equal to *1.e-7* * [.14830897738546 -.04830307526257 -.20219407067329] which together with principal-axis rotation via "evec" enables validation of the top curve on the left of Figure 6.

Additional data will now be presented to enable an accuracy evaluation for the affine fit to the preceding tabulation of pre-quake coordinates. The deformation vector obtained for that day was the product 1.e-9 multiplied by [-0.456365 -5.20928 4.77305 3.19895 -13.2300]

A set of fitted coordinate increments u is formed through premultiplying the 5×1 deformation vector by this matrix:

0.2075	0.1566	0.0510	0.1961	-0.0152
0.0273	0.0381	0.0107	-0.0218	0.2820
0.1942	0.2346	0.4288	-0.0505	-0.0089
-0.1007	-0.0002	-0.1005	0.3453	-0.0267
0.0481	0.0269	-0.0212	0.0000	-0.0003
0.3420	-0.0003	0.3417	0.0996	0.0176
-0.1939	-0.0225	-0.1714	0.1607	-0.0124
0.0224	-0.0137	-0.0361	0.0031	-0.0405
0.1591	-0.0337	0.1254	0.1697	0.0301
0.0113	-0.2693	0.2805	0.3954	-0.0306
0.0551	0.1142	0.0591	0.0375	-0.4851
0.3916	-0.4035	-0.0119	-0.2778	-0.0492
0.1639	0.1852	-0.0213	-0.0300	0.0023
-0.0042	-0.0087	-0.0045	-0.0258	0.3336
-0.0297	0.2775	0.2477	0.0211	0.0037
-0.5881	-0.3105	-0.2776	-0.2267	0.0175
-0.0316	-0.0901	-0.0585	0.0433	-0.5594
-0.2245	-0.4653	-0.6898	0.2749	0.0487
0.1682	0.1868	-0.0186	0.0257	-0.0020
0.0036	-0.0003	-0.0039	-0.0260	0.3365
0.0255	0.2799	0.3054	0.0184	0.0033
-0.1513	0.0150	-0.1663	0.0002	-0.0000
0.0000	-0.0350	-0.0351	-0.0021	0.0269
0.0002	0.0224	0.0226	0.1646	0.0292
0.0869	0.0020	0.0849	-0.4517	0.0349
-0.0629	-0.0450	0.0179	-0.0003	0.0035
-0.4472	0.0029	-0.4443	-0.0841	-0.0149
0.2573	0.1682	0.0892	-0.1269	0.0098
-0.0177	0.0011	0.0188	-0.0234	0.3029
-0.1257	0.2520	0.1263	-0.0883	-0.0156
0.1389	-0.1111	0.2500	-0.2882	0.0223
-0.0402	0.0126	0.0527	0.0155	-0.2002
-0.2854	-0.1665	-0.4519	-0.2476	-0.0438

The accompanying plot shows, in cm, RSS migrations and backtrace-reconstructed coordinate residuals in ECEF.

Figure 9's largest residuals, "BTW" encouragingly, occur at a landmark *other than* that with largest migrations. Also, RSS migrations and reconstructed coordinate residuals in principal axes rather than in ECEF produced subplots somewhat (but not dramatically) better than Figure 10. From material already presented it could be anticipated that

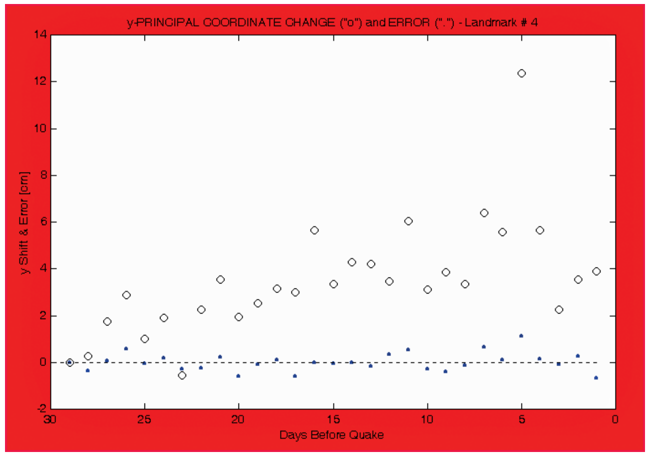

Figure 8: Example of desired performance (y-coordinate of Landmark 4): Low residuals ("•") with larger migrations ("o")

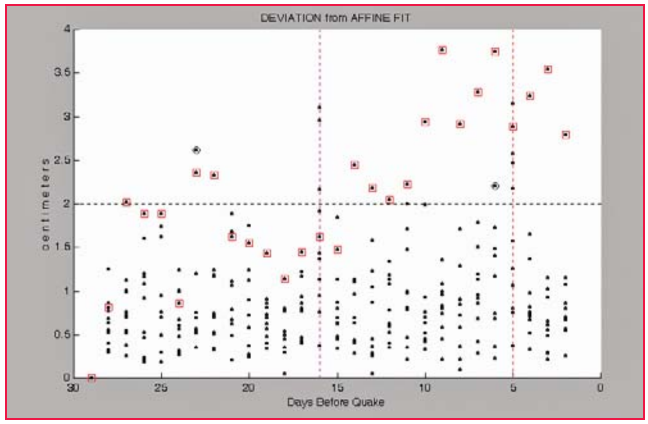

Figure 9: Complete set of RSS residuals (near-epicenter values enclosed within a square), approx. 2 cm dispersion range

- individual (*x*, *y*, and *z*) components exhibit some traits that are more impressive (small residuals with relatively large migrations) and some that are less so (migrations and residuals both near *2* cm).
- the former are reminiscent of Figure 8 while the latter call to mind the "bunch of dots" perception.

Many other plots were generated whose presence here might add only marginally to material already shown. Post-quake time histories, for example, show poorer adherence to affine modeling – even with the "Day #**I**" reference moved to the first day after the quake. Additional prospects, seeming to warrant further attention even pre-quake, were noticed but not yet fully pursued. Of primary importance at this stage of presentation is a clear understanding of what the affine fit – based on evidence obtained thus far – offers toward quake anticipation. In brief, the least squares fit appears to

- provide awareness of the larger landmark excursions while "middling and muddling through" the smaller and, in the process of doing that,
- suggest clues in advance regarding time and location

Limits of time and space now prompt a shift of attention to listing of areas deserving extended investigation.

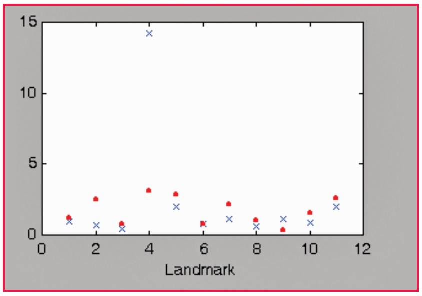

Figure 10: Migrations ("x") and residuals ("•"), Day "-5"

Recommended future extensions

Insight gained thus far easily justifies advocacy for accumulating a data base from experience, by applying morphometrics to several more known quake histories. That recommended effort could employ both variations in, and extensions of, methods used here. The former (i.e., variations) could include assembling data blocks with modifications in content. While an increase in station density has obvious practical limitations, there could be multiple runs with different station selection criteria (based on association with tectonic plates, full encirclement of epicenter, etc.). Measurement count could be increased by longer pre-quake duration, higher measurement frequency, and/or integration [3] with a low cost IMU for short term motions. Also it must be recognized that errors in recorded coordinate values are correlated (above-horizon geometry alone is sufficient to guarantee that) – but they are processed as if they were independent. The way to quantify that effect is to record individual satellite measurements instead of coordinates [7] with weighting based on (potentially nonuniform) individual measurement accuracies.

Extensions of procedures used herein could account for

- alternate shape state formulations, with other pairs of axes chosen to have the independent expansions
- strength of materials (bending for shear states, tensile and compressive strength for expansion / contraction)
- inhomogeneous tectonic plate composition, irregular cross-section geometry
- other items (static friction, partially abutted surfaces • • •).

Other possible extensions, probably with lower priority at present, might include pursuing the TPS further, addition of deformations with spatial nonlinearities (i.e., nonlinear only w.r.t. position but not nonlinear w.r.t. the state – in analogy with linear estimation for a quadratic or cubic polynomial fit), or other non-affine deformation patterns (e.g., twist). In any case, highest value will be attached to models showing consistency with empirical quake data, and experience gained from analyzing past histories will offer predictive capabilities for the future.

Further promising applications (with suitable modification): ***tsunami prediction*** [8] and ***aging infrastructure***.

Conclusions

For investigation of earthquakes based on their affine degrees-of-freedom, methodology of another field –anatomy – is highly relevant. Instead of designated landmark sets coming from a group of patients, here they are associated with a series of days (e.g., from several days before to several days after a quake). Each landmark set is then subjected to a sequence of procedures thoroughly familiar to anatomy experts and succinctly reviewed herein.

Physiological studies of affine deformations in current practice ironically lack a crucial feature; they concentrate heavily on two-dimensional representations. While full affine representation is very old, its inversion (i.e., optimal estimation of shape states from a given overdetermined coordinate set) has heretofore been limited to 2-D. Immediately then, extension was required for adaptation. The fundamentals still remain applicable, however, as indicated by several plots presented in this paper.

A serendipitous discovery, verifiable from data included here and easily applied to other quake histories, calls for further investigation. Sensitivity to incremental rotations, formulated from Procrustes representation even without computing affine deformations, jumped beyond range before returning to "normal" – twice, well in advance of the quake (i.e., first by sixteen days and subsequently by five days). That behavior, plus other results shown herein, exhibit encouraging prospects for warnings in advance of quakes (and potentially, tsunamis or infrastructure failures).

Acknowledgment

Prof. Frank van Graas and Ryan Kollar of Ohio University provided all landmark data for this investigation. Without their diligent acquisition and validation of the data, none of the results presented here could have been generated. They join me in appreciation of the opportunity to pool our efforts with others in this field, toward reducing the danger to those ar risk from earthquakes.

References

[1] F. van Graas and R. Kollar, "Processing of GPS Station Data for Prediction Algorithm Analysis of the 2011 Tohoku Earthquake," ION Pacific PNT 2013.

[2] J.L. Farrell, Integrated Aircraft Navigation, Academic Press, 1976 (now in paperback; – *http://jameslfarrell.com/published-books-gnss-aided-navigation-and-tracking*

[3] J.L. Farrell, GNSS Aided Navigation and Tracking, Amer. Literary Press, 2007 (*http://jameslfarrell.com/wp-content/uploads/2012/03/GPSINS.pdf*).

[4] D.F. Rogers and J.A. Adams, Mathematical Elements for Computer Graphics (2 ed), McGraw-Hill, 1990.

[5] M. Zelditch et. al., Geometric morphometrics for biologists: a primer, Academic Press, 2004, ISBN 0-12-77846-08, pages 137-142.

[6] F. Bookstein, "Shape and the Information in Medical Images: A Decade of the Morphometric Synthesis," Computer Vision and Image Understanding, v66 n2, May 1997, pp. 97-118.

[7] J.L. Farrell, E.D. McConkey, and C.G.Stephens, "Send measurements, not coordinates," ION Journal, Fall 1999, pp. 203-215

[8] R. Nakasone and N. Kubo, "New Approach for Tsunami Detection Based on RTK-GNSS using Network of Ships," ION-GNSS-12, Nashville TN, 2012.

"Business momentum has been rising each month during 2013"

Says **Francois Erceau, General Manager, GeoInstruments, Spectra Precision Division**

Ashtech invests heavily in the development of cutting-edge technology. Please elaborate.

The Ashtech name has always been synonymous with original, innovative technologies and ground-breaking solutions, and we continue that tradition within the Spectra Precision business. The focus of our innovation is evolving, as we aim to deliver products that are simpler, easier to use and easier to deploy across a wider range of users.

How does the OEM business of Ashtech contribute to the overall business of Spectra Precision?

The Ashtech-branded GNSS boards and Integrator-ready GNSS receivers are now managed as part of the Trimble Integrated Technologies (OEM) business. That business sells not only GNSS technology but also digital radio technology and other integrator offerings including software and services. The Ashtech GNSS OEM portfolio nicely complements the existing Trimble "BD" range of GNSS boards, providing integrators with a wide range of options and capabilities to choose from.

How has been the journey so far after formation of Spectra Precision's GeoInstruments business?

During 2011, our main focus was on merging the Spectra Precision/Nikon and Ashtech teams, with emphasis on R&D, Sales, Marketing and Operational Support functions. During 2012 we streamlined our product portfolios and expanded the range of products available to our combined sales channels. We also rationalized our back-office systems to take advantage of our parent corporation's powerful business infrastructure.

To reflect the maturity of our integration, we have recently renamed the combined Spectra Precision/Nikon/Ashtech business as the "GeoInstruments" business area within Spectra Precision.

How significant is the accessories market share for Spectra Precision?

We offer an extensive range of accessories tailored for our Spectra Precision and Nikon branded surveying and construction products. Additionally, we have within Spectra Precision a vast array of more generalized accessories under both the Spectra Precision and SECO brands. Overall, our accessory portfolio is the broadest in the industry: bar none!

What are the new product and solution scheduled for release this year for different market segments?

We are continuing to streamline our product portfolios, replacing older products and closing the few gaps that remain. With our combined organization we can leverage greater R&D resources and the steady stream of product announcements already this year demonstrate our commitment to meeting our customers' needs. In January we launched the NPL-322 entry-level reflectorless total station family, and in March we introduced the world's lightest GNSS RTK receiver, the ProMark 700. We continue to refine our Survey Pro field software, with a new version shipping in April. And our new Layout Pro solution for construction has recently been updated with support for the FOCUS 30 robotic total station.

As they say in show business, "there's plenty more to come".

How your products like ProMark and Epoch address the users' needs in GNSS surveying?

Our ProMark and EPOCH GNSS systems are designed by surveyors, for surveyors. We integrate all the features you're going to need in the field (including cellular and UHF communications), and we leave out anything that's just going to get in your way. Simply Powerful is our promise and these sophisticated but easy-to-use GNSS systems are precisely that.

Tell us about the key features that help FOCUS® 30 Total Station to meet the users' requirements.

FOCUS 30 is an amazing instrument: it boasts innovative tracking capabilities, high speed and superlative accuracy. Coupled with the Ranger 3 data collector it ensures productive surveying all day, every day.

In addition to our Survey Pro software for intensive professional surveying applications, we now offer the FOCUS 30 robotic instrument with Layout Pro software, for construction layout applications. The introduction of mechanical total stations revolutionized the way layout is done, but there's a quantum leap in productivity when you use a robotic instrument to do layout. The digital CAD design literally leaps off the page and onto the ground, enabling rapid, accurate construction immediately after the design has been signed off.

How do you look at the marine and avionics applications?

Within the GeoInstruments business, our sophisticated ProFlex 800 GNSS receiver is frequently used by marine integrators.

In the avionics arena the main product offerings are the Ashtech-branded boards and systems promoted by the Integrated Technologies business of Trimble. The avionics industry has extremely specialized requirements, for example FAA certification, and meeting those requirements requires specialized attention and business focus.

What is Spectra Precision's preparation to the challenges of multi-GNSS scenario?

As you know, we have been at the vanguard of GNSS-centric technology from the beginning, and indeed we are the only mainstream GNSS vendor offering GNSS-centric technology today. Our Z-Blade GNSS engine allows all available GNSS signals to be used interchangeably, eliminating reliance on any specific GNSS system. So, for example, our Z-Blade GNSS receivers are capable of operating in GLONASS-only or Beidou-only mode if required.

The next few years will bring a plethora of new GNSS signals, and the days of inadequate coverage would seem to be gone, at least for those GNSS receivers that can make use of the new signals without being hampered by old restrictions (such as a reliance on at least 4/5 GPS satellites for example).

Which market segments are your main targets for GNSS receivers?

Within the GeoInstruments business, our main GNSS target markets are land surveying and mobile mapping (GIS). For the most part these markets are addressed with out-of-the-box solutions, but in some regions we work with 3rd party software companies to deliver localized solutions. And we continue to work with a range of special applications such as waste management and on-machine control.

Our mobile mapping products are used in a wide range of applications, from natural resource management to urban asset management and utilities.

What are the marketing challenges faced by you at Spectra Precision?

Our products are sold under the Spectra Precision (all portfolios) and Nikon (optical portfolios only) brands. We continue to acknowledge our history through selective use of the TDS (Tripod Data Systems) brand for surveying software in the US market, and the "Powered by Ashtech" moniker which indicates GNSS products with embedded Ashtech technologies.

Do you think Ashtech is better positioned now after its acquisition by Trimble?

Ashtech customers now have a far wider range of products to choose from, spanning not just GNSS technologies but also optical instruments, lasers, radio and cellular communications technology, software and services. So clearly we are better positioned to serve the needs of those customers, both now and in the future.

For our staff, of course, there is also a much wider range of opportunities as we are now a part of a much larger organization, with many career options and the chance to participate in major projects that would have been beyond our capabilities as a smaller private company.

How do you synergize your marketing and branding strategies of various products?

We sell products under a number of brands, the broadest being Spectra Precision itself. The Nikon brand is of course rightly famous and is carried by many of our optical products. And while SECO is our primary brand for generic surveying and construction accessories, we also sell rebranded accessories to many 3rd parties and many of our competitors pay us the compliment of selling our accessories with their own surveying and construction products.

How does Spectra Precision address the requirements for user-friendly and cost effective GIS/GNSS solutions?

Spectra Precision is focused on providing solutions that are easy to learn and use, and which are robust and reliable in the toughest conditions. So our R&D investment is focused around those product virtues, particularly those of simplicity and reliability. Some vendors rush to add more bells and whistles to their products, often making them more complex (and frequently doing so without actually adding features of real value to mainstream customers). We prefer to put our effort into features that serve to make our customers more productive, from the moment they open the box.

How do you see the growth of surveying and mapping market in near future?

The last 5 years have been more difficult for construction and surveying markets worldwide, with the multi-wave financial crisis causing a slowdown in market activity across the globe. But we see plenty of bright spots emerging and most of our key markets are now growing again, even those in Western Europe. Business momentum has been rising each month during 2013 and with the fit between our product portfolio and our customers' requirements now better than ever, we are confident that we're going to continue helping those customers work productively and accurately in future.

Cadastral reform project in South Korea

The main purpose of this research is to propose the establishment of cadastral reference network based on the WGRS, and to make a fundamental plan which is unified into one national reference point

Kang, Sang-Gu
Spatial Information Research Institute, Korea Cadastral Survey Corp., Seoul, Korea

Kim, Kyung-Il
Spatial Information Research Institute, Korea Cadastral Survey Corp., Seoul, Korea

Kim, Tae-Hoon
Business Director Korea Cadastral Survey Corp., Seoul, Korea

In order to solve the underlying problem, Korea MOLIT (Ministry of Land, Infrastructure and Transport) enacted a special act on cadastral resurvey, proclaimed this on 16 September 2011. With the implementation of this special act from 17 March 2012, a CRP (Cadastral Renovation Project) has been being promoted in earnest. Therefore, a multi-purposed control network should be firstly constructed to promote effectively on the CRP. The system of reference point for CRP has to be promoted by applying unified network of reference point based on the WGRS (World Geodetic Reference System) rather than applying by dual-reference points through surveying and cadastral surveying. MOLIT has performed a demonstration project for Digital Cadastral Construction from May 2008 to the end of 2012 for introducing the WGRS to the field of cadastral surveying and promotion of CRP. As a result of this project, in 2009, satisfactory 1600 reference points which have the accessibility, availability, good line of sight (sky-visibility) among cadastral triangulation point and cadastral control points distributed in nationwide were selected to maintain the cadastral control point based on the WGRS. The cadastral control network for CRP is composed of national reference point and cadastral control point. A national reference point is re-classified as CORS and MCP (Multi-purposed Control Point). It is judged that the cadastral control point firstly organizes the 1st grade network based on re-estimated reference point, and then, it is necessary for cooperation plan with the cadastral control points which are newly installed for the introduction of WGRS by a local autonomous entity.

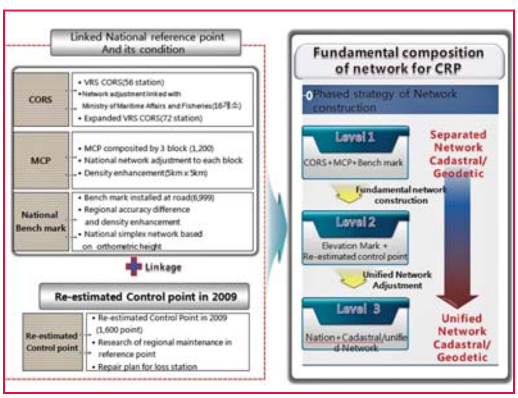

Figure 1: Linkages of national reference point

To do this, the present investigation estimates some factors such as the present state of reference point, installation history, positioning accuracy, and utilization with regard to current-operating CORS, MCP and re-estimated reference point (RRP). Finally, this investigation proposes the construction of a cadastral control network based on the WGRS for promoting CRP well-matched to the Korean topography.

Research contents and methodology

The main contents and methods of this investigation are as follows; firstly, the current statue of the CORS and reference point with regard to national reference point is analyzed. Secondly, the formation of cadastral control point, previous maintenance history and characteristics, utilization, and the correlation of national reference point, performance differences are analyzed for the connection with cadastral criteria. Thirdly, the linkage with national reference point is established for the efficient use of the construction of cadastral control network based on the WGRS.
On the basis of previous estimation, the distribution density of reference point analyzed for CRP; contribute to systemize the construction of cadastral control network and utilization based on WGRS.

New strategies for construction of cadastral control network

National reference point and associated procedures

Currently, MOLIT has announced new government guidelines that cadastral confirmation survey should comply with the act of Surveying, Hydrographic Survey and Cadastre in terms of conducting cadastral survey based on WGRS. At the same time, due to the social disarray induced by the transformation of WGRS, the exception regarding the postponement is made until 31 December 2020. The cadastral control point based on the WGRS for CRP should be organized around the CORS, MCP, re-estimated reference point, instead of connect with previous cadastral control point. Every performance of cadastral survey is generally presented by the point based on the WGRS, it should be connected with national reference point considered as the basic format for the WGRS. In this research, the linkage of national reference network is constituted by correlatively connecting with 56 CORS, 1200 MCP network, and 1600 re-estimated reference network for the construction of cadastral control network based on the WGRS.

Density analysis by using distance between points

The cadastral control network proposed in this investigation used the CORS and MCP as a criterion among national reference points, and the cadastral control point re-constructed in 2009 is the key-point of investigation in terms of the construction of reference network. In order to analyze the national placing density of cadastral control network based on the WGRS, it should be inevitably estimated the network configuration and distance between points from CORS, MCP, and the re-estimated reference point. In this investigation, an acceptable accuracy has been computed by error propagation law; this is conducted in accordance with the order of primary consideration.

Analysis on distance between points included island

First of all, the distance between points located within the triangulation control network which has been constructed by CORS, MCP, and re-estimated reference point included at Jejudo, Ulleungdo, Dokdo, and Baelyeungdo has been analyzed. Figure 2 shows the analysis of distance between these points.

Table 1: Analysis on distance between points per reference point

Network Configuration	Region	Analysis
CORS +MCP	Throughout Nation (included Island)	Maximum distance Minimum distance Average distance
CORS + re-estimated reference point		
MCP + re-estimated reference point		
CORS +MCP+ re-estimated reference point		
CORS +MCP	Land (excluded Island)	
CORS + re-estimated reference point		
MCP + re-estimated reference point		
CORS +MCP+ re-estimated reference point		

The triangulation control network has been formed with the connection of CORS and MCP located throughout Korea. As a result of the analysis of the distance between points within this network, the maximum distance is approximately 430km while the minimum distance is about 0.005km. This investigation is to check the overall distribution of simplex network and distance between points. It is enable to be evaluated as just the geometric value because this is not applying for real surveying project. The average distance is about 14km.

Analysis on distance between points excluded island

The case of the exception for the reference point located in the main island such as Jejudo, Ulleungdo, Dokdo, and Baelyeungdo, the analysis on the distance between points of simplex network is shown in Figure 3.

In the comparison of distance between points from simplex network organized CORS and re-estimated reference point on the main land, the maximum distance is approximately 180km and the minimum distance is around 0.233km. From these, the average distance is calculated by 9.8km.

Establishment of the standards of acceptable accuracy

The accuracy of current cadastral surveying

The accuracy in cadastral surveying is classified with mainly three factors; the accuracy for primary control point surveying, surveying method and surveying equipment, the accuracy

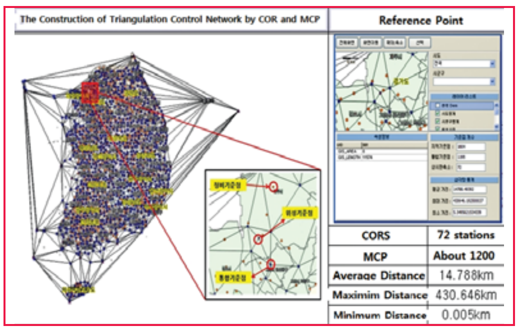

Figure 2: Analysis on CORS and MCP

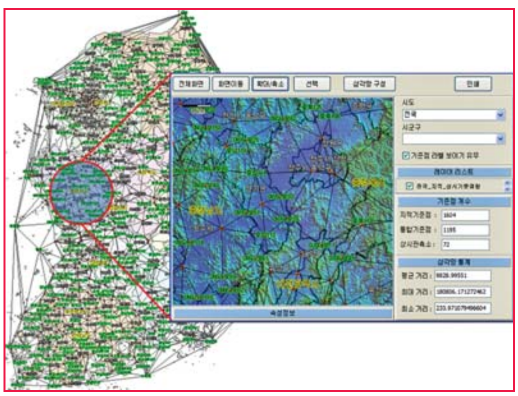

Figure 3: Analysis on the distance of CORS and re-estimated reference point in main land

to restore the boundary on a map to ground boundary point, and the accuracy for maintenance of ground boundary point. The accuracy points mentioned above should have the consistency.

Numerical analysis to accuracy

When conducting on cadastral control point, the accuracy is defined to total station surveying. This is based on lateration, the accuracy to distance should be suitable for ±(5mm+5ppm) regardless of the type of cadastral control point.

However, the currently introduced surveying equipment has the higher accuracy than the one announced in regulation. Therefore, accuracy will not be an issue any more unless the artificial error is induced. When analyzing the accuracy of the distance, with the assumption of 2km average distance between cadastral triangulation control point, if the accuracy ±(5mm+5ppm) of the enforcement regulation of cadastral surveying is applied.

$$e = \pm\sqrt{5^2+(5\times10^{-6}\times2\times10^6)^2} = 1.2mm$$

If the location of cadastral triangulation control point from CORS is determined with the accuracy by ±1.2cm, the accuracy of this point must have the level of ±3.2cm. Moreover, if in the conjunction with MCP, the accuracy by the level of ±4.4cm can be determined. In the case of cadastral supplementary control point, its accuracy can be considered by ±0.7cm under the same standards. If the location is determined through those connected with CORS, its accuracy is ±3.1cm. And then, in the location determination connected with MCP, the accuracy by level of ±4.5cm can be expected.

New construction of cadastral control network for CRP

Establishment of the standards

The unification between the geodetic and cadastral control point for successfully promoting of CRP in the near future should be firstly carried out adjustment of the unified network. To do this, systematic implementation strategies are required as follows.

Analysis on regional reference network (Kangwondo)

The worst limitation, in terms of the construction of reference point, is the application of GPS affected on environmental effect. In the particular case of a forest or urban place, the construction of reference point network should be restricted due to the deficiency of the tracking number of the satellite. With the consideration of this viewpoint, the configuration density of reference point and surveying technique are considered depending on the characteristic of topography. The Kangwon province having the highest forest density is performed to the most frequently survey as the combination of GPS and TS. Due to this, it can be expected that this province will carry forward a CRP among the latest target area.

Considering the regional features, the average distance between reference points is approximately 8.7km, followed by the Article 9 (Section 1 No.2) of enforcement regulation on cadastral surveying, when using a precise macro meter having a standard deviation of more than ±(5mm+5ppm), the accuracy can be calculated as follows;

$$e = \pm\sqrt{5^2+(5\times10^{-6}\times8.7\times10^6)^2} = \pm4.4cm$$

Also, in the case of CORS or MCP, the accuracy is estimated by around 5.3cm. In accordance of the regulation of triangulation surveying the accuracy of the GPS receiver, ±(5mm+1ppm× D), the accuracy of GPS receiver itself can be estimated by about 1cm, when measuring from CORS or MCP, the accuracy is about 3.2cm, in the case of

Table 2. Analysis on accuracy in cadastral control point

The type of cadastral control point and distance between points	Average distance(d) and composition of reference point	Accuracy
Cadastral triangulation control point (2~5km)	·if d=2km, ·CORS+Cadastral triangulation control point ·CORS+MCP+Cadastral triangulation control point	Accuracy : ±1.2 $\sqrt{3^2+1.2^2}=\pm3.2$ $\sqrt{3^2+3^2+1.2^2}=\pm4.4$
Cadastral supplementary control point (1~3km)	·if d=1km, ·CORS+Cadastral supplementary control point ·CORS+MCP+Cadastral control point+Cadastral supplementary control point	Accuracy : ±0.7 $\sqrt{3^2+0.7^2}=\pm3.1$ $\sqrt{4.4^2+0.7^2}=\pm4.5$
Cadastral supplementary control point (< 500m)	·if d=0.05km, ·CORS+cadastral supplementary control point ·CORS+MCP+cadastral control point+cadastral supplementary control point	Accuracy : ±0.5 $\sqrt{3^2+0.5^2}=\pm3.0$ $\sqrt{4.5^2+0.5^2}=\pm4.5$

Table 3: Establishment of cadastral control network based WGRS

Promotion strategies	Contents
Data research to the performance of re-estimated reference point	• cadastral control point, the quality control of GPS measurement and conducting conformance test • classification of data issued in accuracy
the construction of cadastral control network for the linkage from CORS/ MCP/ re-estimated reference point	• Design unified network with re-estimated reference point by considering the density of CORS, MCP
composition between reference points and GPS surveying	• back-up surveying for the precise linkages with CORS, MCP
adjustment of national unified network and application plan for CRP	• Carrying out national network by using precise network software such as GIPSY-OASIS/QOCA, GAMIT/GLOBK • new construction of reference point through density analysis by MCP • application plan for CRP

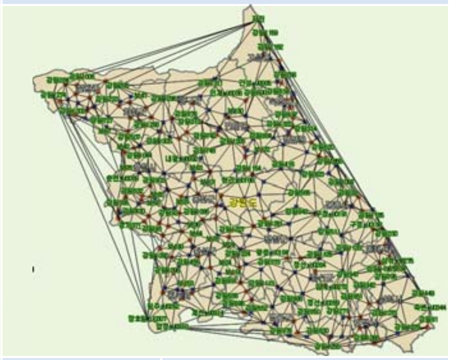

Distribution status of reference points		Composition of triangulation control network	
CORS	12	Max. distance	About 121.5km
MCP	175	Min. distance	About 0.12km
re-estimated reference point	228	Avg. distance	About 8.7km
Accuracy analysis to average distance	Accuracy		±(5+5ppm)=about4.4cm
	CORS→ re-estimated reference point		$\sqrt{3^2+4.4^2}$ =about 5.3cm
	MCP→ re-estimated reference point		
	CORS→MCP→ re-estimated reference point		$\sqrt{3^2-3^2+4.4^2}$ =about 6.1cm
	Notice: separation between available region for GPS surveying and not		

Figure 4: Analysis on cadastral control point in Kangwondo

the successive measurement of CORS, MCP and re-estimated reference point, the accuracy by 4.4cm is estimated.

New model for reference network

The most important factor with regard to construction of new network is the standards for accuracy notified special act on CRP. In the article of this act, in the acceptable range to linkages of performance test, the cadastral control point is ±3cm, and boundary point is ±7cm. According to the estimation of the average distance between points of simplex network organized from regional CORS, MCP, and re-estimated reference point, Seoulsi and 6 metropolitan cities have a shorter average distance than that of other provinces. Even the number of reference point is small compared to the area. The average distance of Seoulsi and 6 metropolitan cities is 6.3km and that of other provinces is 8.5km. Overall average distance is around 7.5km. The distance of the metropolis is longer by 1.2km than overall average distance. When conducting on the measurement of cadastral control point with average distance of 7.5km, the accuracy of theodolite itself is estimated as follow.

$$e = \pm\sqrt{5^2+(5\times10^{-6}\times7.5\times10^{6})^2} = \pm3.8cm$$

In order to meet a acceptable accuracy (±3cm) of special act on cadastral resurvey, it can be implemented by reducing the distance between points with additional installation of reference point. As be calculated this theoretically,

$$\sqrt{5^2+(5D)^2} = 30mm,\ D = 5.9km$$

Therefore, the average distance of network which consists of CORS, MCP, and re-estimated reference point should be within 5.9km to meet the acceptable accuracy in terms of construction of reference network. In the placing density of current MCP, 1200 reference points is installed through the grid of 10km×10km throughout Korea. Due to the increase of the convenience follow-up surveying, the placing density should be raised by the grid of 5km×5km.

However, the installation location of new reference point should be collected by considering on some factors such as geometric strength, the facilities of use, accessibility and convenience of follow-up surveying.

The analysis which is calculated in this investigation is just ot theoretical value; the distance between points of new installed point may be changed if regional distribution of reference point and its characteristics are reflected. However, the result of this investigation is able to utilize as fundamental resources in terms of construction of reference point. The average distance was calculated to 15 different regions. With regard to accuracy from these points, MCP was determined from the performance of CORS, sequentially MCP was applied to determine the re-estimated reference point. On all occasions, the accuracy by 7cm is not exceeded.

Conclusion

Firstly, the simplex network is constructed by linking 72 CORS, 1200 MCP, 1600 re-estimated reference point distributed throughout Korea. As a result of distance between points through simplex network, it can be identified that the average distance included island is about 9km; the average distance excluded island is around 7.7km. The acceptable maximum accuracy is estimated based on ± (5mm+5ppm) accuracy of theodolite surveying. The regional density of reference point should be increased for CRP.

Secondly, the distance between points of metropolis and each province is calculated for considering regional characteristics. The average distance of metropolis is 4~5km, however, the case of reference point installed in forest or agriculture region such as Junlanamdo, Kyeongsangnamdo, Kanwondo has the lower density composited by 8~9 km average distance. Since acceptable accuracy is set-up at ±3cm for CRP with consideration on the national average distance of 7.5km, the installation density of reference point should be increased.

Thirdly, the average distance of network which consists of CORS, MCP, and re-estimated reference point should be within 5.9km to meet the acceptable accuracy in terms of construction of reference network. When considering the convenience of follow-up surveying and installation density of MCP the reference network of 5km×5km is suitable, but to do this, it can be estimated that more than 2000 reference points are necessary. And also, the installation location of new reference points should be collected through the facilities of use, accessibility and convenience of follow-up surveying.

Table 4. Analysis on accuracy to average distance of reference points

Accuracy analysis to average distance (cm)	Accuracy	±(5+1ppm)=about 1.0
	CORS→ re-estimated reference point	$\sqrt{3^2+1.0^2}$ =about 3.2
	MCP→ re-estimated reference point	
	CORS→MCP→ re-estimated reference point	$\sqrt{3^2+3^2+1.0^2}$ =about 4.4

Table 5. Characterization of reference points in metropolis and each province

Region	Regional average distance	
Kangwondo	about 8.7km	
Kyeongkido	about 7.6km	
Kyeongsangnamdo	about 8.7km	
Kyeongsangbukdo	about 8.4km	
Kwangjoosi	about 5.6km	
Daegusi	about 5.7km	
Daejeonsi	about 7.5km	
Busansi	about 5.2km	
Seoulsi	about 4.5km	Minimum
Ulsansi	about 7.8km	
Incheonsi	about 7.8km	
Junlanamdo	about 8.6km	
Junlabukdo	about 7.6km	
Chwoongchungnamdo	about 8.7km	
Chwoongchungbukdo	about 9.6km	Maximum
	Overall average	**about 7.5km**

References

Alfred K., P. J. G. Teunissen, 1996, GPS for Geodesy, Springer.

Jantien Stoter and Peter van Oosterom, 2003, Cadastral Registration of Real Estate Objects in Three Dimension, URISA Journal . Vol. 15, No. 2.

King, R. W. and Bock, Y., 2003, Documentation for the GAMIT GPS Analysis Software, release 10.1, MIT, Cambridge.

Mekik, C. and Can, O., 2010, An Investigation on Multipath Errors in Real Time Kinematic GPS Method, J. Sci. Res. And Essays.

Tomoji T., 2010, Development of an Open Source Multi-GNSS Data Processing Software, 2nd Asia-Oceania Regional Workshop GNSS 2010.

Outdoor mobile field robot navigation

This paper proposes a low-cost field robot capable of short-range field navigation, obstacle avoidance, color identification and spraying. Multiple micro-electro-mechanical sensors (MEMs) and multiple micro-controllers using a multi-layer fuzzy logic decision scheme were integrated to guarantee the autonomy of the mobile robot. Readers may recall that we published the first part of the paper in previous issue. We present here the concluding part

Chung-Liang Chang
Ph.D., Associate Professor, Department of Biomechatronics Engineering, National Pingtung University of Science and Technology, Taiwan, R.O.C.

Bo-Han Wu
Master, Department of Biomechatronics Engineering, National Pingtung University of Science and Technology, Taiwan, R.O.C.

Yong-Cheng Huang
Graduate student, Department of Biomechatronics Engineering, National Pingtung University of Science and Technology, Taiwan, R.O.C.

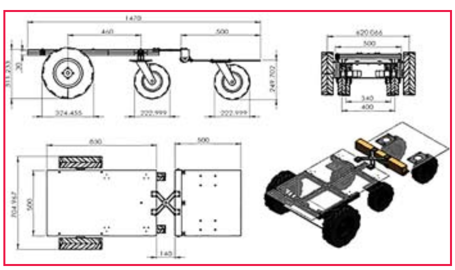

Figure 7. Overview of proposed robot base design

Hardware and software implementation

This section presents the structure of a mobile field robot, including a robotic base and an embedded circuit board design.

Robotic base

The design of a mobile field robot must take into consideration its environment, the weight it carries and the size of the mobile robot. We utilized the speed difference between the two front wheels for steering control of the robot. The coupling mechanism design increases both the carrying capacity and the scalability. The robot, including its two motors and four wheels, weighs approximately 17.2 kg. With the addition of an embedded board, spraying module, battery and tow tractor, the total weight increases to 29.2 kg. The overview of the proposed mobile field robot is shown in Figure 7.

Sensors

The key components of the mobile robot were: the platform on which all modules are mounted; the multiple micro-controllers; the power circuitry; the motor controller; and finally, the sensors, including GPS module, Hall-rotary wheel encoders, an inertial measurement unit (accelerometer and gyroscope), an electronic compass, temperature/humidity (T/H) sensors, a laser range finder and a color sensor.

GPS module

The GPS module was produced by Parallax Inc. using an internal chip from the SiRF III chipset. The chip features 20 parallel satellite tracking channels for fast acquisition of National Marine Electronic Association (NMEA) data for vehicle navigation, telemetry or experimentation. The GPS module can interface with a microcontroller or even a personal computer (PC) via USB.

Odometry

Optical encoders are capable of calculating the distance a vehicle has traveled and provide information related to the direction of the vehicle. In this paper, optical encoders were used for secondary measurement of the vehicle's heading and distance traveled. This data was used to supplement the information from the accelerometer and the gyroscope. Note that the sensors combined with IMU circuitry are capable of yielding far more accurate results and provide a more accurate estimation of the location of vehicles.

Electronic compass

This module employs a simple high-precision electronic compass capable of acquiring angles relative to North, according to the intensity of the magnetic field using BASIC programming language. In addition, it can make corrections anytime and internally set the desired bias angle to ensure that the vehicle maintains a fixed direction. The angle of direction is measurement in degrees functioning to determine the direction of a target and support the GPS module and IMU to accurately estimate the direction.

Accelerometer and gyroscope

Determining the relative location of autonomous vehicles is also necessary. The use of encoders to count wheel rotations is a good way to calculate distance and direction to determine the current position. Nevertheless, this method is susceptible to several sources of error including wheel slip. If wheels slip on the surface, the extra rotations result in inaccurate measurements of distance and direction. This paper used an accelerometer and gyroscope to determine the direction of the vehicle and support the GPS module to provide more accurate information. Semiconductor MMA7455L 3-axis digital output accelerometer is a low powered, micro-designed sensor capable of measuring acceleration along its X, Y, and Z axes. The module has a built-in ADC, low-pass filter, and selectable sensitivity range of ±2g, ±4g, or ±8g, which is perfectly suited to the proposed vehicle.

LISY 300AL is a single-axis high-precision gyroscope, capable of providing a maximum detection rate of 300 degrees/sec, maximum speed of 88 Hz and MEMs design of minimum size. Internally, the gyroscope sensor generates approximately 1.6 V on its analog when it is motionless. The output of LISY300AL was fed into a 10-bit analog to digital converter (ADC), with a high-speed (4 MHz) serial peripheral interface (SPI) and the signal pins capable of operating at 3.3 V and 5 V.

Laser range finder

The laser range finder is produced by Parallax company. The sensor module uses propeller 8-bit core chip and CMOS camera to detect the range, which is between the laser center to the object. The maximum measure range of laser range finder is 2.4 meters.

Color sensor

The color sensor employed in this paper was the TCS230 module produced by Parallax. The module integrates many electronic components, including a TAOS TCS 230 RGB sensor chip, a lens, and two current-regulated white light emitting diodes (LEDs). Those sensors are capable of measuring all visible colors and performing the task of color identification through BASIC Stamp.

Embedded circuit board design

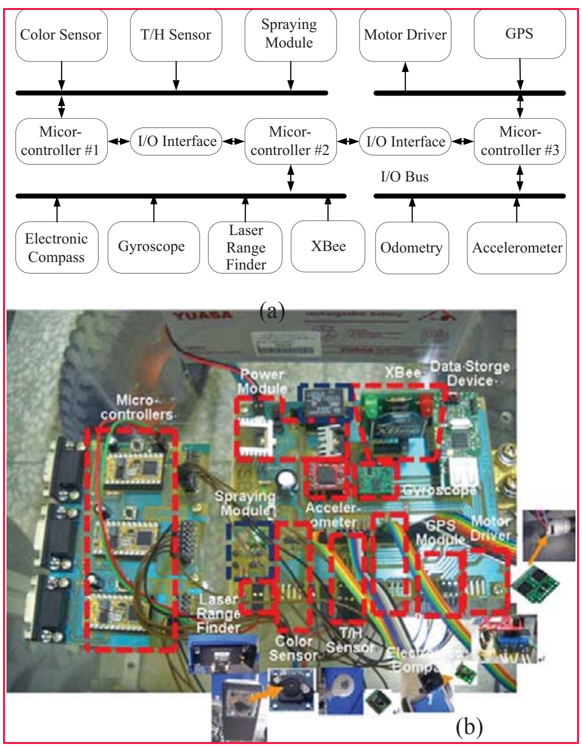

Figure 8. Embedded multi-sensor fusion circuit board; (a) Block diagram of proposed system; (b) Embedded circuit board

Figure 8(a) illustrates a block diagram of the mobile robot system, comprising three micro-controllers, MEMs and spraying module. The first controller (micro-controller #1) receives digital data from the color sensor, T/H sensor, and spraying command. The second controller (micro-controller #2) receives signals from the gyroscope, electronic compass, laser range finder, and 2.4GHz XBee module (IEEE 802.15.4 protocol). The third controller (micro-controller #3) receives the GPS navigation data, accelerometer data and odometer data. Figure 8(b) shows the appearance of the embedded circuit board.

The GPS module is produced by Parallax Inc., using an internal chip from the SiRF III chipset. This module can interface with a microcontroller or even a personal computer (PC) via a Universal Serial Bus (USB) port. The IMU comprises an accelerometer, a gyroscope and an electronic compass, to collect data related to orientation and positioning. The laser range finder is used to detect the distance between obstacles and the mobile robot, to avoid collisions and maintain a fixed distance. A color recognition sensor is used for spraying. Data collected by each of the sensors is sent to the microcontrollers, where preliminary data processing is conducted. Data is stored with a heading identifier (ID) to identify the type of data. Thus, in writing the navigation algorithm, the micro-controller core was tasked with calculating the current location, based on the data collected from each sensor, and then conducting a dead-reckoning algorithm relative to the location of the target.

A simple command setup enabled the motor control board to change the speed of the direct-current (DC) motor at any time and receive data related to the current status of the motor, such as speed or direction data. The control board could handle a maximum current output of 30 A and a maximum input voltage of 35 V, with the provision of an internal 10 KHz pulse width modulation (PWM) current control, which was very convenient for the implementation of motor-speed control.

The proposed technique was implemented in an embedded system, which consisted of three micro-controllers (see Figure 8(b)). The programs of ‘color identification,’ ‘T/H detection’ and ‘spraying’ were written into the first micro-controller. The programs for ‘target tracking,’ ‘obstacle avoidance,’ and ‘decision mode’ were written in the second micro-controller. The programs for ‘motor controller’ and ‘dead reckoning’ in the navigation system were written into the third controller. The initial navigation parameters of the robot (including GPS data, landmark map, initial position of robot, obstacle position, relay position, etc.) and the fuzzy rule table were written to expand the memory module. Before the experimental testing, each sensor module had to be tested to determine whether it could operate properly *a priori* in its integration with the mobile robot system. After the evaluation of the individual components was completed, the fusion-system testing began.

Experiment results and discussion

In many ways, farms are well-suited to autonomous guidance systems. For instance, the workspace does not change; landmarks may easily be installed in the corners of a field, which is then regarded as a stationary space. Crops usually include the same plants in the same places, which can be easily identified. In addition, with regard to such simple tasks as spraying and plant detection (identification), information given through the surrounding environment suffices to meet the same positioning demands. Even though the disadvantages of using mobile robot in greenhouses outweigh the advantages, adequate strides in related fields have been taken to justify proceeding with development. Therefore,

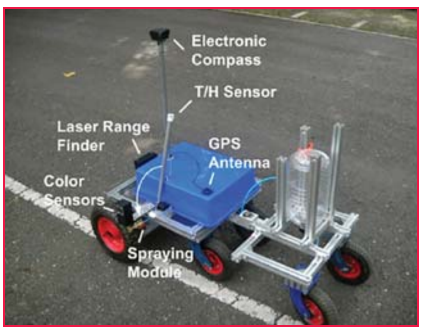

Figure 9. The appearance of the mobile robot

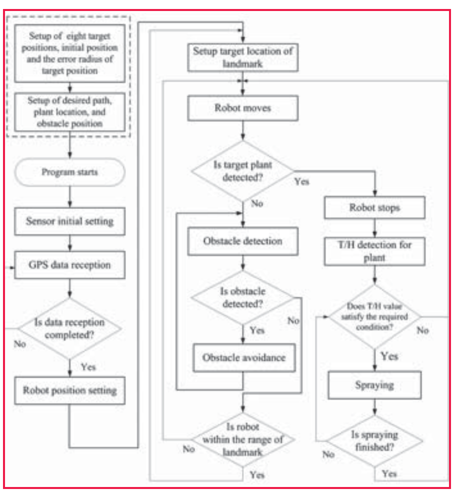

Figure 10. Flowchart of the navigation program in the mobile robot system

the content of this section describes the testing process and evaluates the system performance of the mobile field robot, as shown in Figure 9. The electronic compass was mounted on top of the mobile robot to avoid electromagnetic interference. The T/H detection device was installed at the top of the water pipe. The servo motor module drives the pipe down, so that the T/H detection device could detect the value of T/H around the plant. The laser rangefinder was installed in front of the mobile robot and could perform horizontal rotation (about 180 degrees) through the servo motor module. Meanwhile, the laser rangefinder could be used for avoiding obstacles.

Testing was conducted in a constructed open area in Pingtung County, Taiwan. There were seven GPS satellites observed in the sky. For movement in an open area, the robot moved around the rectangular lawn in front of an apartment building at the National Pingtung University of Science and Technology (NPUST), Taiwan. The selected test area was approximately 20 meters square. The circumference was 70 meters, with '**A**' as the starting point and '**B**' as the endpoint. In this experiment, the locations of eight points were measured and recorded in advance within the robot's system. A path was then planned with these points known beforehand. The robot moved clockwise based on the planned path, with each corner set at 90 degree angles. It was necessary to set a range to determine whether the robot reached the landmark, and the radius was set at 1.25 m. As long as the robot was within range of the landmark, it was considered to have reached the target landmark and could move toward the next.

Two experimental scenarios were developed and demonstrated. In the first scenario, the functionality of autonomous navigation of the mobile robot was tested. The second scenario involved the mobile robot navigating in the presence of obstacles and plants. The user could set the desired path, the locations of obstacles and plants and the color value. A flow chart of the program is shown in Figure 10.

The data (desired color range, planned path and location of landmarks) needed to be recorded before starting the mobile robot. Once the robot detected the desired color values, the T/H sensor module was then used to detect the temperature and humidity values around the plant. If the T/H value was below the desired value, the spraying operation was performed using that module. In addition, the laser range finder was employed to detect obstacles in front of the robot. After the process of color-detection and obstacle-avoidance, the mobile robot moved toward the nearest landmark. If it moved into the range of the landmark, the next landmark became the desired location.

Scenario 1: Autonomous navigation test

The purpose of this experiment was to test the ability of the mobile robot to follow a path, using its IMU component or its electronic-compass module in conjunction with the GPS module and the odometer, through a proposed scheme. In the setup of the experimental parameters, it is necessary to calibrate the gyroscope and accelerometer before its use. This could be done at startup by making sure the gyroscope and accelerometer are

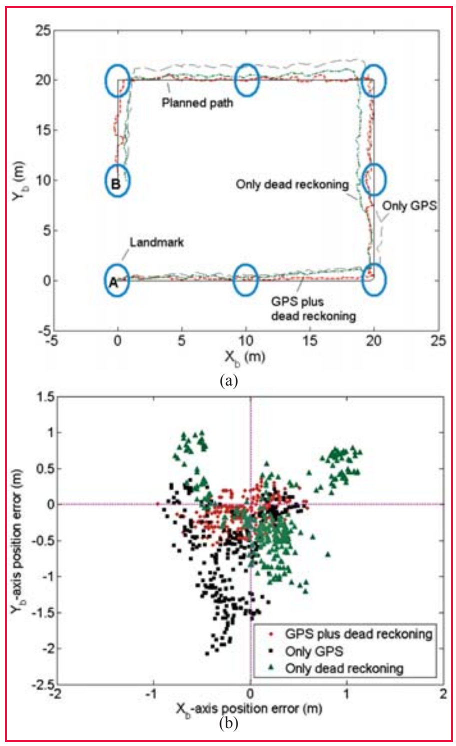

Figure 11. Test results of Scenario 1 on the grass area; (a) Movement path of robot; (b) Positioning error of robot navigation

Table 6. The positioning error with/without GPS module (Scenario 1).

Method	Positioning error (m)			
	X_b		Y_b	
	Mean	Variance	Mean	Variance
Only GPS	0.83	0.27	1.27	0.29
Only dead reckoning	1.16	0.16	0.89	0.14
GPS plus dead reckoning	0.46	0.19	0.39	0.15

stationary, whose output values (500 data) are sampled using the analog-to-digital converter (ADC) to obtain the root mean square value. This value could be acquired each time at startup, or it could be stored after initial calibration. The variance of a_{X_a} and a_{X_b} are 0.23 m/s^2 and 0.26 m/s^2, respectively.

The sampling time of the GPS module was setup as 1 Hz. The output of the data rate of the accelerometer and the bandwidth of the gyroscope were 125 Hz and 88 Hz, respectively. This would be fine for a typical mobile robot navigation. After the adjustment of the parameters, the GPS module performed a 'warm start,' and then the navigation program started to calculate the position of the mobile robot. As the mobile robot reached the set range of landmarks through its navigation system, it began to search for the next landmark. Figure 11(a) demonstrates the experimental results under different combination method on the grass area. From Figure 11(b), it can be seen that the average position errors of X_b-axis direction and Y_b-axis direction with GPS plus dead reckoning method are 0.46 m and 0.39 m, respectively, which produces high accuracy in positioning.

The average positioning error with and without (w/o) GPS is demonstrated in Table 6. By referencing the estimated position and the desired positioning data, the position error could be calculated. From Table 6, it can be seen that the adoption of the GPS plus dead reckoning method with the multi-layer fuzzy control system resulted in the lowest degree of positioning error.

Scenario 2: Obstacle avoidance and plant-spraying tests

The second scenario was conducted in a field in which the robot was required to spray and identify a colored object when it moved. When objects were detected, the robot stopped and sprayed them, using a sprayer. While moving, the robot followed a planned path. Colored objects were placed near the planned path to test the detection performance of the robot. The functions of obstacle avoidance and plant spraying were tested in the outdoor environment. The information regarding the locations of obstacles and plants were recorded in the memory module of the mobile robot beforehand. After 10 testing, the average path of motion for the robot was as demonstrated in Figure 12 (The blue dot represents an obstacle; the pink dot represents the plant.). As is shown, the robot stopped where it encountered the colored objects and sprayed them. In addition, the mobile robot avoided the obstacle successfully. However, the robot could not reach into the range of landmarks successfully.

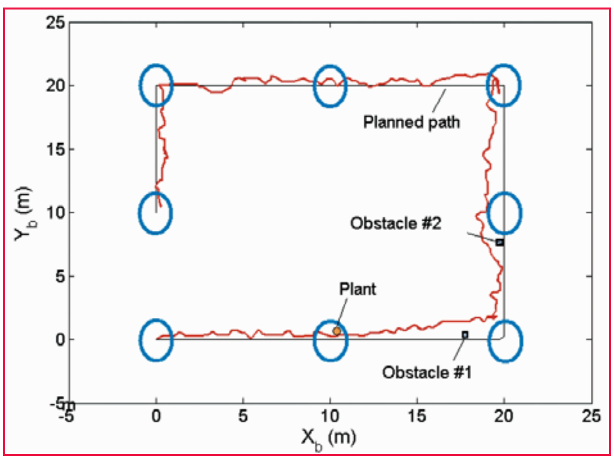

Figure 12. Moving path of the robot in the presence of the obstacle and plant

Conclusions

This paper proposes a low-cost micro-controller, in conjunction with an MEMs component, to produce a multi-sensor embedded navigation system for implementation in a small mobile field robot. A multi-layer fuzzy system was utilized in robot navigation, spraying and obstacle avoidance. The use of the proposed decision scheme could enhance the positioning accuracy in both X_b-axis and Y_b-axis directions, to 0.46 m and 0.19 m with 0.2 m/s, respectively, over uneven pavement and with known landmarks.

In addition, the positioning accuracy effect of the mobile robot in the presence of different sensor combinations was analyzed. Although the adopted IMU sensor resulted in accumulated positioning errors, the precision of positioning was significantly improved by adjusting the scale factor and bias using software and odometry. The navigation system was equipped with GPS/IMU/odometry sensors, which could cause the positioning errors in both the X_b-axis and Y_b-axis directions to reach **0.76 and 1.43** meters, respectively, at a speed of 0.2 m/s. Overall, this system was flexible in combining different sensor elements for navigation, and also allowed for installation of the different brand sensors to an embedded board.

The proposed mobile field robot succeeded in detecting and accurately identifying objects, as well as spraying, during experiments in a field. The total cost of the robot was approximately US$ 930, including design, implementation and system integration, which was inexpensive considering the quality of the components used. This study implemented the concept of a multi-sensor embedded system in a mobile gardening robot, which may be valuable for future applications in greenhouses.

Acknowledgements

This work has been supported by the National Science Council, Taiwan, Republic of China, under grant NSC 101-2221-E-020-018.

J-shield “Don’t Worry! ... Be Happy!”

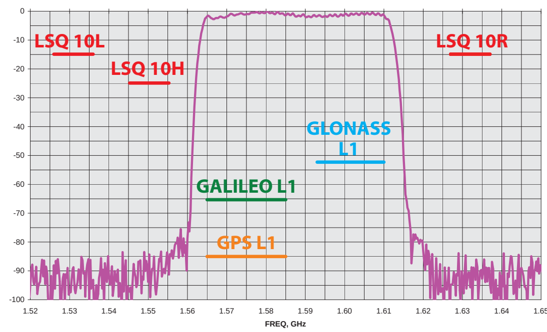

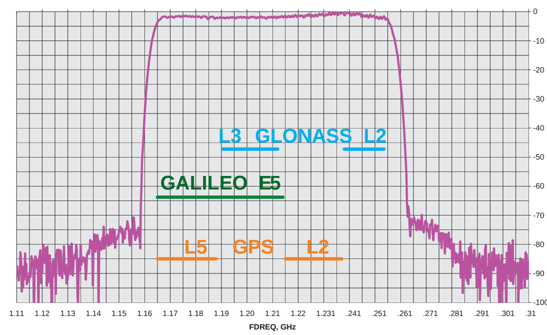

Don’t worry if FCC ever authorizes any broadband wireless near GPS L1 band.

We already have proven technology to protect not only against this particular one, but against all similar systems in all GNSS bands. It is implemented and fully tested option in our GNSS antennas. Our nation can have full benefits of high precision GNSS (no performance degradation at all) and full benefits of broadband wireless.

Those who cannot innovate in Silicon Valley,

lobby in Washington DC by misinforming the FCC and the Congress about the status of technology and about the status of existing receivers in the field.

TRIUMPH-1

Fully integrated package

An elegant, rugged, light, and hermetically sealed box accommodates **all GNSS and modem electronics and antennas.**

Spectrum

The unique

spectrum analysis

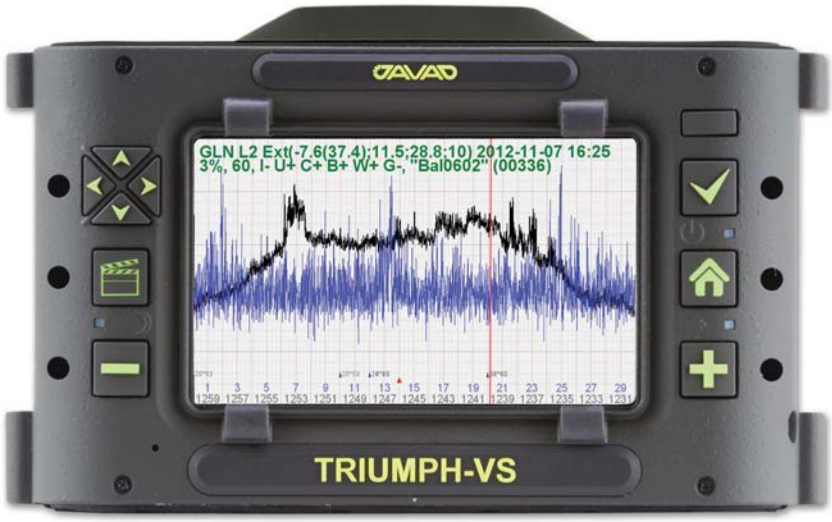

and

interference

detection/protection

features in our

GNSS receivers.

Visual Stakeout

Target point itself

View your target point on the **TRIUMPH-VS** screen and **walk towards it** to stake it.

Each of our

6 Parallel RTK Engines

employs different algorithms
to calculate solutions

and
the weighted average of them
provides the **most robust,**
accurate
and **fastest** results.

Survey with Lift&Tilt

You don’t need to look.
You don’t need to touch.

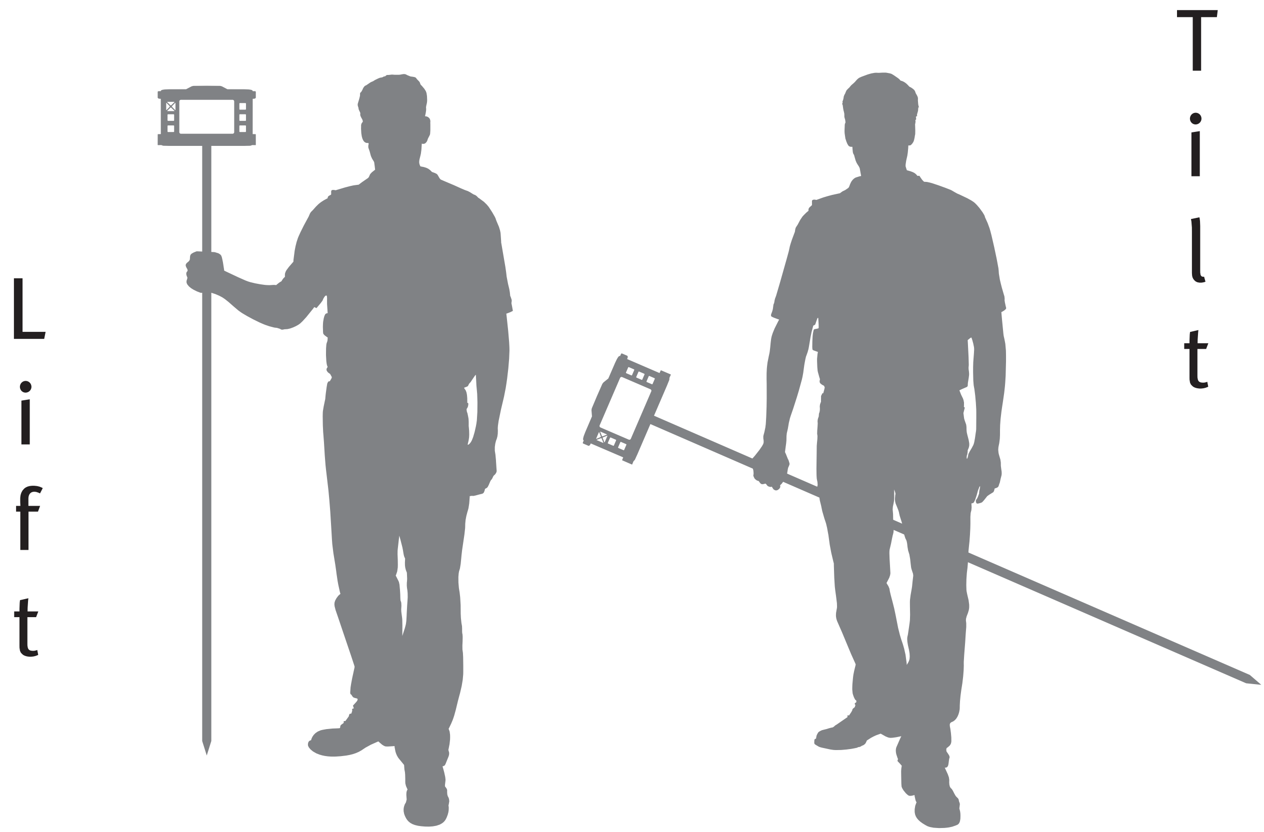

TRIUMPH-VS brings this new

revolution to surveyors

All-in-one

TRIUMPH-VS

GNSS receiver that combines high performance **216-channel GNSS receiver,** all-frequency **GNSS antenna,** and a modern featured **handheld.**

Software

Complete software suite for survey, GIS and control.

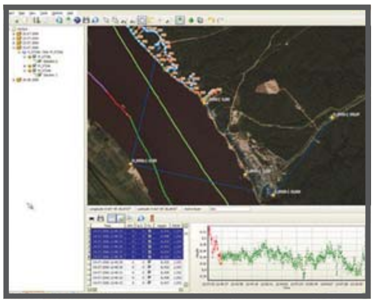

Justin has full range of features for geodetic and surveying tasks.

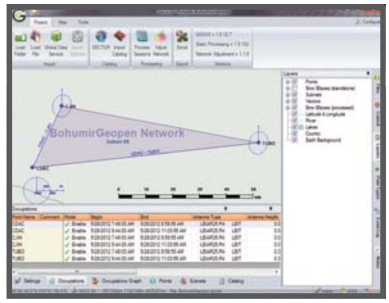

Giodis is a sophisticated and easy to use geodetic software.

NetView is an application to easily control JAVAD GNSS receivers.

NetHub is a Windows® application for controlling GNSS receivers developed by JAVAD GNSS, INC.

see the latest at **www.javad.com**

The Himalayan Tsunami in Uttarakhand

Thousands of people died in Uttarakhand, a state in North India due to devastating floods and landslides in June 2013. What went wrong?

Anoop Nautiyal
Social and political commentator, former Chief Operating Officer, 108 Government emergency services, Uttarakhand

Uttarakhand is in absolute shambles. Disaster, with most people calling it more manmade than natural, has exposed the fragility of this beautiful yet ecologically vulnerable region. Untold and unimaginable damage has been done with surging rivers and flash floods bringing death and destruction together. Glaring manmade gaps and inefficiencies have been identified and highlighted. All of this has left the State, its people and the citizens of our country traumatized.

Crisis in focus

As Uttarakhand completes its first month after the recent disaster, it is amply clear that this is a huge moment of grave crisis for the State. This tragedy, the biggest ever to hit Uttarakhand, has brought into sharp focus the fierce debate around environment, development, governance, politics and disaster management. Though the fury of nature has been unprecedented, many questions are being asked about the role of the State Government. These questions, based on equal doses of frustration, sadness and anger, are mainly being raised about the lack of disaster preparations and the development model pursued by the Government.

By now several facts are well known. The Uttarakhand Disaster Management Authority, constituted under the Chairmanship of the Chief Minister, has had no meetings since the past six years. Successive CAG reports have made scathing remarks on the lack of disaster management preparations in the State. Indiscriminate mining, haphazard urbanization, rampant cutting of trees and forest covers, use of dynamites for road construction, encroachments, buildings, hotels, guest houses and travel lodges on the river bed, too many hydropower projects, changing river courses, poor structural safety – this was clearly a Himalayan tsunami waiting to happen. Locals in the affected areas claim that this is only the trailer of the massive destruction that is lurking in this region of the country. Many others are calling it a ‘Human Tsunami’.

Challenges being faced

Uttarakhand is prone to frequent flash floods, landslides and cloud bursts. The mountain ranges are relatively new. Climate changes are impacting rainfall and cloud bursts in the Himalayan region, which have already seen increase in temperature that are 2-3 times higher than the average global temperature rise of 0.9 Degrees C. Against this background, the State has miserably failed to develop any systems of early warning, forecasting and disseminating rainfall and landslide related information. Technology is available that can predict cloud bursts at least three hours in advance, but no such sophisticated equipment is used in the State. In 2008, the Doppler radar system was sanctioned for Uttarakhand but due to lack of coordination between NDMA, IMD and the Uttarakhand Government it was not purchased.

There are other challenges too. Uttarakhand is politically as fragile as its mountain ranges. With six different individuals holding the Chief Minister’s position during the last 13 years, since the formation of the State in 2000, the average tenure of each has been two years.

Uttarakhand has miserably failed to develop any systems of early warning, forecasting and disseminating rainfall and landslide related information. Technology is available that can predict cloud bursts at least three hours in advance, but no such sophisticated equipment is used in the State

This has resulted in lack of continuity and failure in getting a firm grip on the issues plaguing the State. These figures look even more ominous when compared with Himachal Pradesh, Uttarakhand's Himalayan neighbor. Himachal Pradesh has had five chief ministers during the past 60 years. Only two, Virbhadra Singh and Prem Kumar Dhumal, have held the reign of the State since the last 20 years.

The political fragility has resulted in ad hoc and unplanned development. Successive governments have failed in creating any sort of medium term or long-term plan or vision for the State. Most decisions appear unconnected and lack coherence. They are mostly random in nature and pander to the demand of the moment. Political instability and inexperience have also resulted in lack of articulation about the firm and correct position to be taken by the State in several matters that are most important for them. Programs and policies are started but often are not completed due to frequent changes. In this scenario, how is sustained development possible?

Who is responsible?

Clearly the major defaulter is the political leadership of the State and the Government of the day. The political leadership in Uttarakhand, with the exception of a few distinguished and sincere politicians, is widely perceived as being either corrupt and/or incompetent. Internal squabbles are hardly leaving any time for senior party leaders to give any quality time for public issues, strategic planning and the long-term development of the State. Just before the massive disasters struck Uttarakhand, five MLAS of the ruling party were camping in Dehradun, the State capital, for few days protesting against their own Government and complaining about the lack of development in their respective constituencies. Bureaucracy is being adversely affected. When politicians frequently complain that bureaucrats are not listening to them and the bureaucrats retort that the politicians do not let them work, the leadership deficit at the highest levels becomes clear and apparent.

Environmentalist accuses U'khand govt of ignoring NRSA report

Accusing the Uttarakhand government of sleeping over a report of National Remote Sensing Agency, noted environmentalist and Magsaysay awardee Chandi Prasad Bhatt today said had the government taken the report seriously "destruction in and around Kedarnath shrine would have been much less horrific".

"The scale of destruction at the Himalayan shrine could have been far less if the state government had paid adequate attention to the report of National Remote Sensing Agency, whose scientists had identified the natural calamity prone areas of Uttarakhand and neighbouring Himachal Pradesh way back in 2001," the Magsasay awardee said.

"The report identifies the areas around Kedarnath including Rambara, Gaurikund, Ghindurpani, and Garuriya, which have been the worst hit in the recent tragedy, as highly prone to landslides and natural calamities," he said.

The report, termed as 'Hazard Zonation Mapping', was prepared by arond 100 distinguished scientists from country's leading research institutes at the initiative of the Indian government and was submitted to the state government in 2001.

"But since then, it has been gathering dust in the offices of district magistrates who have done precious little to implement the recommendations of the panel," the environmentalist alleged.

The expert panel had recommended a host of measures for the calamity sensitive area of the state and neighbouring Himachal Pradesh including planned mining, bio-technical measures for channelisation of water in the catchment areas of rivers near Kedarnath, afforestation of Rambada and Jungle Chatti areas, soil conservation and slope modification measures in Gaurikund besides construction of retention walls in Hanuman Chatti which have all been severely damaged in the deluge.

"Had even five per cent of the recommendations of the panel been implemented, the scale of destruction in and around the Himalayan shrine would have been much less horrific," he said.

www.business-standard.com, June 23, 2013

The Government is now staring at mammoth challenges. They need to act and act quick on multiple fronts. As Uttarakhand continues to grapple with inclement weather affecting relief operations, the next set of action items need to be ready. Detailed impact assessment of affected areas and the learning's from this tragedy need to be documented. Immediate compensation of the locals needs to be finished on a war footing. Roads and bridges need repairs. Hospitals and food supplies need strengthening. Livelihoods dependent on the Char Dham Yatra need to be restored. It's a long list that requires serious planning, coordination, strategy and execution.

What next?

Where does Uttarakhand finally move to from here? This is not only a time to mourn, but also to reflect and create a blueprint for its future and destiny. The policy makers can move in any of the two directions – either follow the path that they have taken earlier and rebuild Uttarakhand on the poor foundation of unscrupulous

and unplanned development. Or take a radical, new path and come up with a unique, innovative and inclusive model of development built on the foundation of modern disaster management techniques and equal concern for the environment and livelihoods. This needs to be the starting point for this development strategy. This path will further require an open mind, belief in science and technology, exemplary leadership and genuine compassion and empathy for Uttarakhand. This is where the whole concept of exceptional leadership comes in.

As the ones who have lost their loved ones try and desperately get their lives back on track and the others limp along, the question that still haunts many is what next? With confidence in the political class at an all-time low, the rehabilitation hopes of the people of Uttarakhand are very low. Though the Government has announced relief and compensation measures, this is clearly not enough to rebuild shattered lives and reestablish broken homes. Much more needs to be accomplished to get things done and to inspire hope for the future. Only exceptional leadership can turn this around.

Defining leadership/ Leadership in question

There are hundreds of leadership definitions. In this time of incomprehensible crisis, the one that appeals the most to me are the famous words of John Quincy Adams, the sixth President of the United States of America - "If your actions inspire others to do more, learn more, do more and become more, you are a leader." The level of leadership that Adams had in mind when he said these famous words is the only level of exceptional leadership that can take Uttarakhand ahead. Politicians and bureaucrats can make plans and announcements, but without exceptional leadership Uttarakhand would continue to lick its wounds and forever feel sorry for itself.

What is the starting point for this exceptional leadership? This has to be leadership that can act quickly and is able to create that sense of extreme urgency. There needs to be leadership that operates on strong principles of alliances and partnerships, and is able to motivate various agencies and institutions to come forward and support the rebuilding of the State. On a sensitive note, this has to be leadership that can deeply feel the pain of the people who have perished and others who have lost everything. Is this level of exceptional leadership possible in today's cut-throat and highly competitive political environment in the State? The non- believer would obviously say no, but in this hour of extraordinary gloom and misery, it is only outstanding actions and exceptional leadership that can heal Uttarakhand and make it move ahead.

What should the leadership in Uttarakhand be doing right now? There are three things to focus on. Creating a vision, communicating that vision and executing the vision is what the leadership should concentrate on. Working on multiple fronts, the leader will have to inspire the millions of 'Uttarakhandis' and the rest of the nation who are all looking up to him for creating a holistic and consolidated strategic long-term rehabilitation and development plan for the State. Integrity, competence and plain old hardwork are just few of the components that are needed for exceptional leadership to have a long-term impact on life and livelihoods in Uttarakhand.

Blueprint of development

Why is creating a vision necessary? In the Cold War era of the 60s, the Americans were lagging behind the Soviets. John F. Kennedy, the then US President, needed a vision to inspire his country and said in the Congress - "I believe that this nation should commit itself to achieving the goal, before this decade is out of landing a man on the moon and returning him safely to the earth." Critics called it fantasy while many others termed it pure lunacy. Kennedy's dream was fulfilled when on July 20, 1969 the Apollo 11 Commander Neil Armstrong stepped foot on moon and said, "That's one small step for man, one giant leap for mankind."

If the Americans could create this extraordinary vision more than 50 years ago, why can't our leadership get inspired and create a vision for the rebuilding of Uttarakhand? Leadership needs to come out with a vision that is clear and articulate. It needs to be simple, inspirational and time bound. In the absence of a vision, as a State, Uttarakhand will once again fail and falter, as it will operate on a day-to-day basis without any long-term goal or plans.

Once the vision is clear, it needs to be clearly communicated and understood. The fulfillment of the vision for Uttarakhand should get utmost priority over everything else that matters. This will require an iron will and the ability to take bold steps at every moment making steady progress towards achieving that vision. The people of Uttarakhand would need to have a deep faith in the vision and would have to truly own that vision. The ability to inspire others would only come with exceptional leadership.

Implementation of goals

How will the vision get fulfilled? This is where the ability to conceptualize, to create institutional frameworks and to deliver outcomes comes in. Creation and communication of the Uttarakhand vision needs to be backed up with execution and results on the ground. The bureaucratic machinery needs to be energized and organized. Deft political handling of opponents within and outside the party needs to be undertaken as a preventive measure. All this would require exceptional leadership.

The cynic, as always, is bound to sneer and call the exceptional leadership dream for Uttarakhand equivalent to making castles in the air, while the optimist agrees to move on the path towards a safer and new Uttarakhand. But for the State to feel optimistic there needs to be an exceptional leader to hold her bruised hands and show her the path. Time alone will tell if Devbhoomi Uttarakhand, the mystical land of gods, legend and lore, was fortunate during its worst times to have had that exceptional leadership.

The use of GIS to forecast tourism demand

This study shows that the full potential of the Huff model has not been recognized yet

Dr Adnan AL-Jaber
Director of Geographical Information Systems MAS Center
Saudi Commission for Tourism and Antiquities, Kingdom of Saudi Arabia

Most applied methods to determine the tourism demand depend on the availability of demographic data, social and economic characteristics of tourists, tourism customs, the quality of tourist activities and facilities, and other foundations such as the capacity of the tourist destination, and its accessibility. So, a tourism site must be designed in accordance with the standards and regulations of great importance in the protection of environment resources, and to develop appropriate plans to meet the expected demand for tourism. The urban planning optimal tourism sites take into account the number of tourists forecast, whenever available accurate data on flow of tourists in the area, which makes tourism development more accurate and logical Because such information can often be unavailable or inadequate to forecast tourist numbers; due to lack of monitoring mechanisms set up, tourists and limitations add to the cost and effort and duration (Ghoneim, 2003). Define and analyze trade areas help forecast tourism flows.

The study goals to achieve the following:

1. Develop an approach for forecasting tourism demand by GIS.
2. Identify the different factors and variables that play an important role of spatial interaction related to tourism demand.
3. Design the necessary database for the model using GIS for a site with real data (Al-Uqair).
4. Implement the automated model, checking its validation, and discussing the possibility of generations.
5. Determine the geographic distribution pattern of the model output and discussing it in the light of the pros and cons of the automated application of the model.

This study uses (ArcGIS Business Analyst), since these systems are designed to analyze and interpret spatially, in addition to calibrating the Huff model to measure tourist numbers through a real case study (Al-Uqair). There are several reasons behind the selection of Huff model in this study. First, the form is theoretically attractive; as the logical underpinning of the model makes sense and the output can be communicated easily and understandably. Secondly, the model is relatively easy to make operational. The necessary computations are straightforward once the values of the variables and parameters are specified. The third reason for the model's popularity is its applicability to a wide range of problems and its ability to predict outcomes that would be difficult, if at all possible, without the model. Despite the general applicability of the model, it has not always been employed correctly. Furthermore, the full potential of the model has not been realized.

Study background

David Huff introduced his model in 1964, which takes into account the number of consumers, the attractiveness of business centers, and the distance and competing commercial centers that predict consumer behavior spatially. Huff model is derived from the theories which are based on spatial analysis which are based on the principle that the prospect of a buying or visiting consumer to a particular site depends on the distance and the attractiveness of the site and the distance and attractiveness of competing sites. This model is used in spatial interactions researches (Huff, 1964).

Trade areas analysis models provide great potential for the formulation and appraisal of geographic business decisions. The Huff model was widely used by business analysts in the public and private sectors as well as academics across the world. The popularity of the model increased with the development of the GIS technology. For example, the model can be used in the field of trade for the following purposes: Assessing market prospects; identifying and analyzing trade areas; assessing market penetration; estimating the economic impact; forecasting consumer choices in shopping; describing the distribution of consumers geographically, and estimating the sales size for the current and potential selling outlets (Huff, 2008). As the case in the trade field where the commercial market penetration is forecast through geographic scope, the same idea could be used to analyze the potential tourism demand, as a commodity subjected to the supply and demand laws.

Using Huff Model for tourism demand estimation

The actual reality theories of tourism demand as indicated in Kafi's study (2008) are as follows: (1) the number of inbound tourists is directly proportional to the number of residents and the intensity of their movements; (2) the number of inbound tourists is directly proportional to the relative attractiveness of the tourism destination; (3) the number of inbound tourists is inversely proportional to the distance to the destination (accessibility). This takes into account the competition factor, where the distribution of potential tourists to competing destinations is taken into account according to the distance. The attractiveness of each competing destination plays an important role in the distribution of the number of tourists, and the attractiveness of any tourist destination depends mainly on the available attracting factors, such as the prevailing natural environment, the type of services available, and the image of a destination that affect the tourist when choosing alternatives. The number of tourism facilities in any tourist destination is a reflection of the attractiveness of this destination; thus, when the attractiveness increases, the destination's facilities increase. In other words, it can be said that tourist destinations that have the greatest facilities have the greatest degree of attractiveness.

Table 1: Tourism Demand Factors List

Factors	Variables	Measuring unit
1. Spatial vicinity	Travel duration (distance)	Hour/ km
2. Area	The developed area comprising tourist facilities (swimming, parks, playgrounds, walkways, camping, resorts, restaurants, and landscape)	Km^2
3. Availability of natural potentials	Availability of natural potentials (along the coast, and such as depth of water, landscapes, terrains, coral reefs, and natural vegetation)	Percentage
4. Surrounding tourism attractions	• Natural sites (mountains, desserts, forests) • Archeological sites • Archeological and historical buildings • Museums • Exhibitions	Number of sites

The Huff model includes many factors and variables affecting the tourism demand which are clarified by previous studies to controllable and non-control variables. The controllable variables could be processed by decision-makers, such as advertisement, tourism packages, prices, and provision of tourism services and infrastructure development. The non-control variables are generally beyond control, such as natural tourism potentials, the archaeological and historical factors, population distribution, distance, and competition. Therefore, the application of the Huff model to forecast the tourism demand requires compiling a list of specific factors. The adopted factors in this study are limited to the significant ones such as spatial vicinity, area, and the availability of natural potentials and other tourist attractions, based on the Hudman study (Hudman, 1980). Both factors are a form of data that will feed the model.

The Huff model is based on the theory that when someone is facing a range of alternatives, the probability of selection is directly proportional to the tangible benefit of that alternative, so the selection behavior is mathematically referred to by (*Pij*). As a result of the alternative selection process, trips are distributed among different tourism destinations. So, the Huff model will be used to measure the distribution of tourists. The factor of distance traveled by tourists to reach the tourism attractions could be used as a variable. And the distance will be considered a main variable in this study, which is measured by the duration of the trip. Given the importance of the time it takes to travel between the places of residence to the tourist destination, the trip duration gives an overview of the accessibility, the traffic volume, and the status and quality of available roads. The tourist site area reflects the attraction power, i.e., the developed area comprising tourist facilities such as accommodation, resorts, restaurants, parks, landscape, and waterscape related to leisure and entertainment. Table (1) indicates a list of tourist demand factors, variables and measuring units, which will be taken into account in this study for Al-Uqair site and competitive tourist destinations. Spatial vicinity factor is inversely proportional with tourists, while the other factors of area, availability of tourism potentials, and the surrounding attractions are directly proportional to the number of tourists.

Mathematical formulation of the Huff Model to forecast tourism demand

A phase of analyzing the tourism demand behavior mathematically by linking the effecting factors and variables. It is called 'the diagnostic since it explains how factors can be linked together through the Huff model. Therefore, the use of the Huff model in this study is as a mathematical equation linking the factors influencing the tourism demand. The Huff model by linking the above mentioned tourism demand factors can be explained by re-explaining the equation number (1) mathematically, as follows:

$$P_{ij} = A_j^{\gamma_1} N_j^{\gamma_2} T_j^{\gamma_3} D_{ij}^{\lambda} / \sum_{j=1}^{n} A_j^{\gamma_1} N_j^{\gamma_2} T_j^{\gamma_3} D_{ij}^{\lambda} \qquad (1)$$

SOUTH
Target your success

High Precision Handheld GPS

India GAGAN era comes

* Work mode and accuracy

SBAS differential mode
(Satellite Based Augmentation System)
(GAGAN / WAAS / EGNOS / MSAS)
----submeter level (with India GAGAN)

Static and Fast Static mode
----mm level

PPK mode
(Post-processed Kinematic)
----cm level (at good condition)
----submeter level (at common condition)

CORS network mode
(Continuous Operation Reference System)
----≤0.5m (Single frequency)
----≤0.2m (Dual frequency)

***** *Accuracy and reliability may be subject to anomalies due to multipath, obstructions, satellite geometry and atmospheric conditions.*

For More Details Contact Us:

India Headoffice

SOUTH PRECISION INSTRUMENT PVT.LTD.
Add: 1108-09-10-11, 11th Floor, RG Trade Tower,Plot No-B-7,
Netaji Subhash Place, Pitam Pura, New Delhi-110034
Tel: +91-11-49995999, 9999999255 Fax: +91-11-45605999
Http://www.southinstrument.com Http://www.southprecision.in

Customer Support Center

Delhi:	+91 9990561049	Ahmedabad:	+91 9971800986
Mumbai:	+91 9766329600	Kolkata:	+91 9007002404
Hyderabad:	+91 9573325063	Chennai:	+91 9650797606
Indore:	+91 9650797607		

Whereas:

P_{ij} = the probability of tourism demand in area (i) frequently visiting the tourism destination (j)

i = area originating tourists (the source)

j = the destination (endpoint)

A_j = area variables in tourism destination (j)

N_j = variables of available natural potentials in tourism destination (j)

T_j = variables of tourism attractions in tourism destination (j)

γ_1 = area variables coefficient

γ_2 = variables coefficient of available natural potentials

γ_3 = variables coefficient of other tourism attractions

D_{ij} = accessibility to tourism destination (j) for tourists in area *(i)* and measuring it with time unit

λ = distance variables coefficient (accessibility (Dij))

n = number of tourism destinations

In this stage, the original the Huff model is being calibrated, tested and validated, as the resulting standard model will be used to forecast the tourism demand in the next period.

The calibration process of the Huff model's variables coefficient requires calculating the data of tourism demand probabilities (ratios), its referred to by (P_{ij}) in equation. The calculations of tourism demand probabilities data are based on choosing appropriate initial values - an approximate weights for key variables coefficients (γ, λ) as a preliminary stage. Therefore, the initial coefficients values are dubious; due to the inability to determine the statistical significance of the variables.

The main two variables (distance, area) influencing tourism demand directly can be identified as follows:

First: The area represents the tourism attraction variable (A_j). And in the beginning, a coefficient value was proposed (γ), which is (1), as neutral value.

Second: The distance represents the tourism direct variable (D_{ij}), the distance between the tourist's place of residence (i) and destination (j). The value of the distance variables coefficient (λ) ranges between (-1) to (- 3) by recommendations from the Huff model (Huff, 2008). (-3) will be used in this study; considering that tourism tours are not services that people need every day.

In this case, Huff model equation is represented as follows:

$$P_{ij} = A_j^{\gamma} D_{ij}^{\lambda} / \sum_{j=1}^{n} A_j^{\gamma} D_{ij}^{\lambda} \tag{2}$$

Whereas:

P_{ij} = the probability of tourism demand in the geographical area (i) frequently visiting the tourism destination (j)

i = area originating tourists (the source)

j = the destination (endpoint)

A_j = measuring area variables in tourism destination (j)

γ = area variables coefficient, initial proposed weight = (1)

D_{ij} = measuring accessibility coefficient between tourism destination *(j) and generating area (i)* measured with time unit

λ = distance variables coefficient of trip duration, proposed weight in this study equals to (-3)

n = number of tourism destinations

So, it is possible to use standard methods like (Ordinary Least Squares) in order to complete coefficients model calibration, where the output of equation (3) is a dependent variable after dividing it on the geometric mean, and all tourism demand factors (attractive and repellent) are independent variables, as follows:

$$\underbrace{\overbrace{\log\left(P_{ij}/\widetilde{P}_i\right)}^{\text{The original Huff model}}}_{\text{Dependent variable}} = \underbrace{\overbrace{\gamma_1 \log\left(A_j/\widetilde{A}_j\right) + \gamma_2 \log\left(T_j/\widetilde{T}_j\right) + \gamma_3 \log\left(N_j/\widetilde{N}_j\right)}^{\text{Attractions}} + \overbrace{\lambda \log\left(D_{ij}/\widetilde{D}_i\right)}^{\text{Negative factors}}}_{\text{Independent variables}} \tag{3}$$

Whereas ($\widetilde{P}_i$, $\widetilde{N}_j$, $\widetilde{T}_j$, $\widetilde{A}_j$, $\widetilde{D}_i$) are geometric means dependent on (P_{ij}, N_j, T_j, A_j, D_{ij}).

You should check the validity of the Huff calibration model results before applying it to the study site (Al-Uqair). This involves five steps - (1) ensuring that all transactions have predictive ability; (2) there should not be co-linearity between the independent variables; (3) verifying the performance of the model, i.e., to make sure that the value of transactions is statistically distinctive; (4) ensuring that all explanatory variables have distinctive statistical implications, which is measured by the identification coefficient (R2); (5) the estimation errors should be naturally distributed, not with high level of statistical implications. All this is done in the light of verification by comparing the results of calibration with real statistical data.

Modified weights of the variables coefficients ($\hat{\gamma}_3$, $\hat{\gamma}_2$, $\hat{\gamma}_1$, $\hat{\lambda}$) result from the Huff model calibration process for the tourism demand variables entered in the model which give more accurate results and closer to the data that have been monitored in the field. After verifying the efficiency of statistical calibration, the model can be applied to forecast the probability of tourism demand in any tourists' exporting area (i), in case of choosing any tourism destination (j), according to the following final equation:

$$\hat{P}_{ij} = A_j^{\hat{\gamma}_1} N_j^{\hat{\gamma}_2} T_j^{\hat{\gamma}_3} D_{ij}^{\hat{\lambda}} / \sum_{j=1}^{n} A_j^{\hat{\gamma}_1} N_j^{\hat{\gamma}_2} T_j^{\hat{\gamma}_3} D_{ij}^{\hat{\lambda}} \tag{4}$$

After statistically determining the criteria, the model can be used to forecast the consumer spending on a certain product provided by the store (j), which is located in a specific geographic area within the study area, according to the following formula:

$$E_{ij} = (P_{ij})(B_i) \tag{5}$$

Whereas:

E_{ij} = the expected expenses from the geographical area (i) to the store (j).

B_i = total expenses in (i).

The total sales in each store in the geographical area can be determined by adding the expected expenses in each geographical area for all stores, according to the following equation;

$$T_j = \sum_{i=1}^{n} E_{ij} \tag{6}$$

Whereas:

T_j = the total expected sales of the store (j).

The market share of each store in the study area equals to the total expected sales of each store divided by the total sales of all stores, as follows:

$$M_j = T_j / \sum_{j=1}^{n} T_j \tag{7}$$

Whereas:

M_j = the market share of the store (j).

Steps of determining the study area

The first and most important step after obtaining the relevant accurate data is to define the tourism impact area as it should be. This stage is very important due to the impact of geographic extension on determining the nature and volume of data that should be collected in addition to any conclusion to be reached based on the analysis of these data. The steps used to determine the impact area are illustrated as follows:

1. Locate Al-Uqair and similar tourism destinations, in addition to the road network and surrounding communities within the study area, which was identified in the third chapter of this study.
2. Determine the tourism impact area which depends on the distance traveled by tourists to reach the destination, assuming that the distance ranges from (100 km) to (400 km). This type of tourism involves a large group of local and regional tourists, and classified as medium-range tourism (Kafi, 2008).
3. Define the borders of the initial impact area, which usually reflects the natural or human barriers that hinder tourism movement between specific areas, and impedes movement between the defined area such as international borders, seas, mountains, and road network.
4. Draw the borders of common areas of influence, and this is the initial approximation to the impact area.
5. Divide the initial impact areas to smaller geographical units through which tourism statistics data could be collected. To determine these smaller geographical units, the previously identified sub-regions are usually used by some entities such as the Department of Census which divides the regions into different levels of spatial details.
6. Obtain the available tourism statistics for each sub-region which include the number of one-day trips, excursions, leisure trips, marine trips, the spending on marine activities, and the required location data (coordinates of latitude and longitude) for mapping each sub-region.
7. Modify the impact area if necessary to reflect the sub-region boundaries.
8. Collect data reflecting the relevant competitiveness of each tourism destination within the impact area such as the area, number of resorts and other tourism attractions.
9. Determine the distances or travel time between the sub-regions and all tourism destinations within the impact area.

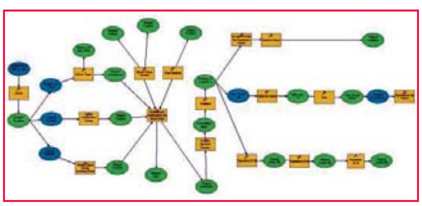

Figure 1: Workflow of forecast tourism demand by model builder.

Application on study case

Geographical location

Al-Uqair is located on the Gulf Sea coast in the Eastern Province of the Kingdom. It is located within Al-Ahsa administrative area. Al-Uqair coast extends between the latitudes (24’ 25º) and (44’ 25º) to the north, and between longitudes (50’ 08º) and (24’ 50º) to the east. It is 50 km long, and 10 km wide inward. See Figure (2).

The tourism significance of Al-Uqair beach lies in its expected role. Its natural components imposed the merging of this beach on the national tourism map in Saudi Arabia, in addition to the likelihood of attracting a large number of visitors and tourists in the future. This means that the development of Al-Uqair beach will relieve pressure on other beaches in the eastern region. Moreover, new investment opportunities, and other economic and social returns are expected (SCTA, 1425).

Figure 2: AL-Uqair Geographical Location

In step (1), Al-Uqair location and other similar tourism destination were determined. There are some tourism centers in the eastern coast which were developed partially or completely, such as Al-Jubail Industrial Corniche, Al-Dammam Corniche, Al-Khober Corniche, Al-Azizia and Half Moon. Similar destinations are located in Al-Dammam, Al-Khober, and Al-Jubail, and can be considered competitive centers for Al-Uqair beach, Figure (3).

Step (2) describes the three competing tourist destinations for Al-Uqair and their areas of impact. They are forecast by circles of (400 km) radius, as shown in Figure (4).

Step (3) shows the final boundaries of the tourism impact area, as shown in figure (5), after being adjusted in accordance to the provincial boundaries. The aim is to facilitate access to the available statistical tourism data at the district level (polygon).

Figure (6) shows the population clusters with over (2,500) people, which is linked to the road network. Their total number reached (232) points, administratively distributed on (16) districts within the borders of the impact area. It is clear that the pattern of the spatial distribution of population points ranges between the clustered and random pattern.

Using cellular representation

By covering the impact area with cellular network helps to calculate the area with square kilometers per unit (cell) in the

Figure 3: Al Uqir and similar tourist destinations

Figure 4: impact areas represented with (400 km) radius circles

Figure 5: Final impact area at which Huff's model will be applied

map. It also helps in measuring the distances required by the Huff model. The selected cell size in this study is (50 X 50) square kilometers, to be compatible with the geographic data representation level at the regional level, and takes into account the spatial distribution pattern of communities. Thus, each cell could contain the largest number of communities, considering the center of each cell to be the distance measuring point to various tourist destinations.

148 cells were excluded because they do not contain any community. So, the total number of cells that contain population clusters is 79 cells within the impact area, as shown in Figure (7).

Concluding the Characteristics of the Tourism Impact Area

Table (2) summarizes the geographical characteristics of the impact area by

Figure 6: Settlements in area of influence.

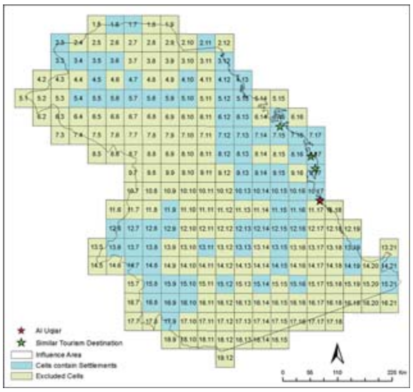

Figure 7: Cells containing population clusters within the impact area

using the cellular model. It is clear that the tourism market options are limited to three destinations competing on an area of 197.500 square kilometers, and 232 population clusters in (16) districts.

Tourist properties may vary among tourism trips exporting provinces depending on the differences in cultural and socio-economic backgrounds, besides the provided recreational activities. Table (3) shows the data of trip source, the number of one-day tourists, the purpose of trips whether for holidays and recreation or voyages; and the tourist spending on marine activities geographically distributed on (16) provinces. It is notable that the pattern of data distribution in the source regions, within the impact area, has no effect on the calibration of the model. However, its role is limited to determining the characteristics of potential tourists.

Analysis and discussion

There is an important factor to determine the impact of any tourist center on the communities which is the availability of other similar entertainment centers. Usually the proximity of tourist destinations to population clusters impacts the beach visitors. Although all destinations seem equal, the central tourism destinations are easily accessed and are likely to attract more tourists compared with other destinations. The attractiveness of tourist destinations, in most cases, is determined according to the variables that can be controlled by development officials as illustrated in the previous chapter. However, the variables used in this case study are limited to - spatial proximity, the area of the destination, and the availability of natural potentials and surrounding tourism attractions.

Table No. (4) clarifies the characteristics of three tourism destinations: Al-Dammam; Al-Khober and AL-Jubail. It is clear that Al-Khober covers the largest area, followed by AL-Dammam and then Al- Jubail. Al- Jubail is featured by the available natural components such as pure sea water, and sandy beaches. Other tourism attractions are equally available in all destinations. Al-Uqair data was limited through the tourism development scheme and the results of the model's coefficients calibration will be applied later.

Table 2: Geographical characteristics of the impact area using the analysis network

Geographical Characteristics	Measurements (quantities, length, area)
North and south	(900) km (the furthest boundary point)
East and west	(850) km (the furthest boundary point)
Total area	(197.500)km 2
Number of population clusters	232
Number of districts	16
Number of impact area cells	227
Number of inhabited cells	79

FOIF Since 1958

It's professional

Suzhou FOIF Co.,Ltd.

For more information please visit our website:
www.foif.com
or email to: internationalsales@foif.com

Or India distributor JANAK

JANAK POSITIONING&SURVEYING SYSTEMS PVT.,LTD

E-mail:janakji@vsnl.com Website: www.janaksurvey.com

Tel: 011-23515400,23515399 Fax: 011-23682185

TÜV CE ISO-9001 DNV CERTIFICATED FIRM Certificate No.QSC-5112

Table 3: Tourists source regions data in impact area in 2007

S	Network code	The district (source) (i)	The number of:				spending on marine activities (SR)
			One-day trips	Tourism trips	Leisure tourism trips	voyages	
1	5.3	Hefr AlBatin	0	173208	38344	980	10257020
2	12.3	AlKhafji	1721	12560	0	1050	535
3	5.1	Qariat AlOlya	0	230	150	89	40125
4	5.12	AlNe'airiah	887	50697	48686	1300	13023505
5	7.15	Al-Jubail	58000	146000	41000	80300	10967500
6	7.17	Ras Tennourah	0	2000	0	1100	535
7	8.16	Al-Qatif	0	7000	0	1294	535
8	8.17	Al-Dammam	2288000	2353000	1601000	1294150	428.267.500
9	9.17	Al-Khober	238000	317000	246000	174350	65805000
10	10.16	Bqaiq	0	3000	3000	1650	10257020
11	11.9	Rmah	0	5000	0	1050	802500
12	11.16	AlAhsa	16000	161000	30000	88550	8025000
13	13.6	Hraimla	0	1016	0	460	535
14	14.7	Al-Deriah	0	360	0	187	535
15	14.8	Riyadh	1506000	3113000	1085000	653730	290.237.500
16	16.1	AlKharj	1000	59000	0	12390	535
Total			**608,109,4**	**071,404,6**	**180,093,3**	**630,312,2**	**0000,000,827**

Source: prepared by the researcher based on SCTA's data 2007

Calibration of the Huff model coefficients to forecast the tourism demand

After collecting the tourism demand potentials' data, which is necessary to calibrate the coefficients of the Huff model, equation (4.10) can be applied which represents the linear version of the Huff model. Table No. (5) shows a sample of regression equation data, including 9 data cells. The third column shows the dependent variable, representing the tourism demand potentials' data divided by its geometric mean. Columns 4-7 show the independent variables arranged successively as follows - distance, area, natural components, tourism attractions, divided by its geometric mean.

Table (6) shows four attempts to calibrate the model. It used another type similar to the multiple regression called the Stepwise Regression, which determines the importance of each independent variable in explaining the change that occurs in the dependent variable. The ratio of change is ordered based on the importance of each independent variable. The order starts from the highest percentage, or the most important variable, and ends with the lowest ratio or the least important variable in explaining the change that occurs in the dependent variable. The fourth statistical model explains the four independent variables (*) (96%) of the variance in the value of the dependent variable (**). The variable of proximity is the most important variable to forecast the attractiveness of the tourism destination selected, representing (69%). On the other hand, the remaining tourism attractions variables have also high statistical significant.

Coefficients estimation

Table No. (7) shows the forecasted coefficients, used as adjusted weights for the tourism attractiveness variables coefficients entered in the Huff model to forecast tourism. The distance coefficient weight ($\hat{\lambda}$) represents the value (-2 ,86), and minus sign indicates diminishing the impact with increasing distance. While the

Table 4: Tourism destination characteristics data (target) in impact area

Tourism destination (target) (j)	Variables data			
	Area (km2) (A_j)	Available natural potentials (%) (N_j)	Number of tourism attractions (T_j)	*Distance (D_{ij})
Al-Dammam city • **Al-Dammam** Corniche	546, 51	55	12	-
Al-Khober district • Al-Khober Corniche • Half-moon beach • Al-Aziziah	864, 159	70	9	-
Al-Jubail district • Al-Nakhil beach • Al-Jubail Industrial Corniche • Al-Jubail city Corniche	007,26	80	10	-
**** Al-Uqair center**	345,509	95	18	-

Source: SCTA, 1430

* distance are illustrated in appendix 2

** proposed services in Al-Uqair tourism scheme, SCTA 1427

Table 5: Partial list of multiple regression equation for set values

Cell number	Tourism destination (j)	Dependent variables	Independent variables			
			Repelling tourism factors	Attracting tourism factors		
		$\log(P_{ij} / \widetilde{P}_i)$ (Percentage/ geometric mean)	$\log(D_{ij} / \widetilde{D}_i)$ (Distance/ geometric mean)	$\log(A_j / \widetilde{A}_j)$ (area/ geometric mean)	$\log(N_j / \widetilde{N}_j)$ (Natural components/ geometric mean)	$\log(T_j / \widetilde{T}_j)$ (Tourism attractions/ geometric mean)
1.6	Al-Jubail	-0,0863	-0,0631	-0,3619	0,0736	-0,0111
1.6	Al-Dammam	-0,0656	0,0221	-0,0648	-0,0892	0,0680
1.6	Al-Khuber	0,1519	0,0410	0,4267	0,0156	-0,0569
1.7	Al-Jubail	-0,0782	-0,0685	-0,3619	0,0736	-0,0111
1.7	Al-Dammam	-0,0683	0,0239	-0,0648	-0,0892	0,0680
1.7	Al-Khuber	0,1464	0,0446	0,4267	0,0156	-0,0569
2.3	Al-Jubail	-0,1058	-0,0501	-0,3619	0,0736	-0,0111
2.3	Al-Dammam	-0,0594	0,0180	-0,0648	-0,0892	0,0680
2.3	Al-Khuber	0,1652	0,0321	0,4267	0,0156	-0,0569

total area ($\hat{\gamma}_1$) represents the value (18,1), the natural components ($\hat{\gamma}_2$) represents the value (12,1), and the tourism attractions ($\hat{\gamma}_3$) represents the value (66,1). The positive variables coefficients indicate an increase along with the increasing variable. After obtaining the results of the coefficients calibration of variables, they will serve as modified weights.

Table 6: Results of multiple regression equation, model summary

The model	Multiple link coefficient	Determination coefficient (RSquare a)	(Model Significance Level)
1	0,8311	0,6907	0,0000
2	0,8422	0,8397	0,0000
3	0,9216	0,9191	0,0000
4	0,9831	0,9665	0,0000

Dependent variable: log (Percentage/ geometric mean)

- Independent variable: log (Distance/ geometric mean)
- Independent variable: log (Distance/ geometric mean) and log (area/ geometric mean)
- Independent variable: log (Distance/ geometric mean) and log (area/ geometric mean) and log (Natural components/ geometric mean)
- Independent variable: log (Distance/ geometric mean) and log (area/ geometric mean) and log (Natural components/ geometric mean) and log (Tourism attractions/ geometric mean)

Table 7: Forecasted coefficients (a,b)

The model	Coefficients		Statistical significance level of Forecasted coefficients
	coefficients values (B)	coefficients calibration error	
1. Distance ($\hat{\lambda}$)	-1,3379	0,0414	0,0000
2. Distance ($\hat{\gamma}_1$)	-1,8636	0,0421	0,0000
Area ($\hat{\gamma}_1$)	1,1682	0,0301	0,0000
3. Distance ($\hat{\lambda}$)	-2,5426	0,0414	0,0000
Area ($\hat{\gamma}_1$)	1,1237	0,0213	0,0000
Natural components ($\hat{\gamma}_2$)	1,4023	0,0434	0,0000
4. Distance ($\hat{\lambda}$)	-2,8695	0,0325	0,0000
Area ($\hat{\gamma}_1$)	1,18100	0,0141	0,0000
Natural components ($\hat{\gamma}_2$)	1,1224	0,0442	0,0000
Tourism attractions ($\hat{\gamma}_3$)			
	1,6622	0,0474	0,0000

It is clear from Table (6) and Table (7) that the fourth model is statistically adequate for prediction, based on the value of the increasing determination coefficient ($R^2 = 0.9665$) This indicates that the tourism demand in tourism destinations depends heavily on the variables given by the model. This is one of the methods used to evaluate the model. In addition, the significance level of the correlation coefficient reached zero (0.00), which is less than the significance level of hypothesis (0.05). Therefore, the regression line matches the data, which is within the limits used by geographers and others when accepting or rejecting the hypothesis that is usually in the limits of (0.50). So, after verifying the efficiency of statistical calibration, coefficients values will be used (adjusted weights) to forecast the tourism demand potential.

The results

Determining Al-Uqair tourism market share

Visual evaluation of the tourism impact area and tourism market share for tourism coastal destinations can be obtained by comparing the equivalence lines of tourism market influence in the destinations before and after adding Al-Uqair destination. Figure (8) shows tourism market influence lines to of Al-Dammam and Al-Khober together before adding Al-Uqair. There is a clear overlap in their influence lines, while Al-Jubail was not added because of its relative faraway distance from Al-Uqair.

Table 8: Tourism market share of coastal tourism destinations before and after adding Al-Uqair

Tourism destination (j)	Market share	
	Before (%)	After (%)
Al-Dammam	62,02	59,66
Al-Khober	28,27	23,33
Al-Jubail	9,7	9,72
	100,00	92,71
Proposed Al-Uqair		7,16

Figure (9) shows the influence lines of the tourism market in the existing tourist destinations after adding Al-Uqair. The differences in the distribution pattern of the lines after adding Al-Uqair is clear. It may be difficult to assess the impact visually, due to the large and overlapping equivalent lines. Al-Uqair share of the current tourism market can be determined.

Table (8) indicates the quantitative estimation of the market share in the three existing tourist destinations within the tourism impact area. It is expected to distribute Al-Uqair market share between four tourism destinations after adding Al-Uqair instead of three tourism destinations. This can be identified through the application of the values of tourism demand potentials on the expenditure data for all source regions. The second column in the table clarifies the tourism market share before adding Al-Uqair. It is observed that the highest share of the current market belongs to Al-Dammam, followed by Al-Khober and then Al-Jubail. While the third column shows the potential tourism market after adding Al-Uqair. It was obtained using equation number (4.5). We note that all destinations have lost a part of tourists' frequent visits. The forecasted loss of tourist destinations is approximately (-7.16%) from current tourists spending which will go to the new destination (Al-Uqair).

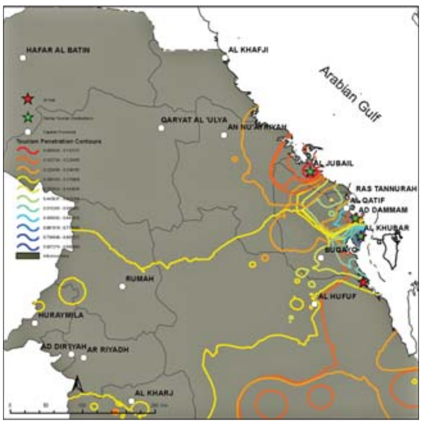

Figure 8: Equivalence lines of tourism market influence around Al-Dammam and Al-Khober before adding Al-Uqair

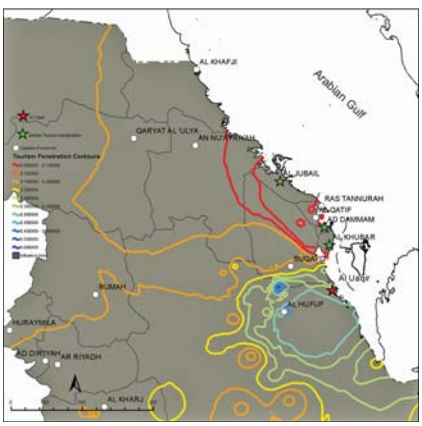

Figure 9: Equivalence lines of tourism market influence around Al-Dammam and Al-Khober after adding Al-Uqair

Conclusion

This study showed that the full potential of the Huff model has not been recognized yet. Adding to the Huff model in the business analyst program in (ArcGIS), the package is a positive step in this direction. There are many applications for this model not only in the field of tourism demand, but in other tourism aspects. For example, analyzing the tourism impact areas, assessing tourism market penetration, estimating the tourism development impact, assessing the tourism environmental impacts, predicting tourist preferences, and finally describing the tourists' distribution patterns geographically. The study recommended the possibility of circulating the application of the model to tourist destinations similar to Al-Uqair in various regions of the Kingdom. The results of the Huff model coefficients calibration are applicable to several tourist destinations without making any changes. Running the proposed model's progress scheme is fast and practical and saves a lot of effort and money, only in case of compliance with the terms and objectives of the model in addition to the required level of details.

References

Arabic references

- Kafi, Mustafa Youssif (2008). Tourism Economics, Syria, Damascus. Dar Al-Redha Publications
- Ghunaim, Othman Mohemmed (2003). Tourism Planning for Comprehensive and Integrated Spatial Planning. Jordan, Dar Al-Safa Publications
- Saudi Commission for Tourism and Antiquities (1425). Tourism Development Strategy for The Eastern Province. Kingdom of Saudi Arabia. Riyadh. Not published
- Saudi Commission for Tourism and Antiquities (2007). Tourism Statistics. First edition. Kingdom of Saudi Arabia. Riyadh. Tourism Information and research Center

Foreign references

- Hooper, H. (1997). Who's Really Shopping My Store? Business Geographies, September, 34-36 (not available online) Hudman, L. E. (1980). Tourism: A shrinking world. Columbus: Grid Inc.
- Huff, David.L. (1963). A Probabilistic Analysis of Consumer Spatial Behavior. William S. Decker.
- Huff, David.L. (1964). Defining and Estimating a Trading Area. Journal of Marketing 28. pp. 34-38.
- Huff, David. L. (2003). Parameter Estimation in the Huff Model. ArcUser, October-December, 34-36
- Huff, David. L. (2004). A Note on the Misuse of the Huff Model in GIS. Retrieved from www.mpsisys.com on January 16.
- Huff, David. L. (2008). Calibrating the Huff Model Using ArcGIS Business Analyst. A ESRI 380 New York St. Redlands. CA 92373-8100. USA

The paper was presented at the Eighth National GIS Symposium in Saudi Arabia during 15 – 17 April 2013.

A Transformational Esri International User Conference

Musician will.i.am Talks Technology, the Urban Observatory Opens, and ArcGIS Online Gets Analytical

It's not every day that a musician inspires a mapmaker.

But that's what happened at the 2013 Esri International User Conference (Esri UC) in San Diego, California. It's where will.i.am, the recording artist and founder of the Black Eyed Peas, helped Katherine O'Brien, GIS coordinator for facilities at the University of North Carolina (UNC), Chapel Hill, make the decision to start mentoring students in how to use geospatial technology.

"I need to go back and work with kids," said O'Brien, who credited will.i.am for inspiring her to get involved.

will.i.am, born William James Adams, started the i.am.angel Foundation in part to support science, technology, engineering, and mathematics (STEM) education in the classroom. He spoke for 30 minutes with Esri president Jack Dangermond about his passion for helping young people get a strong STEM education, including learning to use GIS.

Prior to their conversation, four 11th-graders from Roosevelt High School in the Boyle Heights neighborhood of Los Angeles, California, demonstrated how they used GIS to analyze data using Esri's mapping software. will.i.am, who grew up in Boyle Heights, arranged for them to use ArcGIS for their school projects.

It's important to be tech savvy and computer literate today, said will.i.am. "Most people don't read or write code, but we all use technology to communicate," he said. See the rest of the conversation at esri.com/events/user-conference.

Transforming India

Esri UC keynote speaker Sam Pitroda, an adviser to India's prime minister on public information, infrastructure, and innovations, outlined India's plan to build a national GIS as part of a public information infrastructure. He said 400 million people live below the poverty line in the country of 1.3 billion and that democratizing information using technology help lift them out of poverty.

Sam Pitroda believes GIS will be critical to turning India into an information-rich society.

The creation of a nationwide GIS platform has begun, with plans to use the technology to tag every physical asset in the country and unique identifications (UIDs) for all residents. GIS would help streamline everything from the justice system to the food distribution system and improve housing and education, Pitroda said. "Our goal is really to empower a billion people with knowledge information, and this is where GIS, we believe, will play an important role," he said.

Transforming Urban Areas

The new Urban Observatory opened at the Esri UC. It uses Esri technology to compare demographic and other information about major cities at the same scale.

Esri president Jack Dangermond welcomes will.i.am to the Esri International User Conference

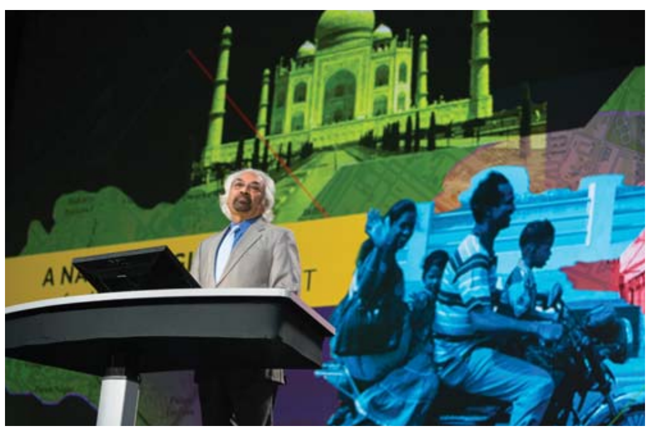

Sam Pitroda believes GIS will be critical to turning India into an information-rich society

A Map Gallery visitor explores the Urban Observatory

It operates both as a live exhibit and at urbanobservatory.org. Participating cities include New York, New York; Tokyo, Japan; Abu Dhabi, United Arab Emirates; Mumbai, India; Paris, France; and Rio de Janeiro, Brazil.

A Map Gallery visitor explores the Urban Observatory.

Transforming GIS

"We need to create a better future with GIS."

That's what Dangermond underscored in his talk about web GIS, which he thinks will be transformational going forward as geospatial technology increasingly becomes easier to use; more accessible; and can integrate big data, 3D data, and much more. "Look what GPS did as a technology. It totally transformed us as human beings so we are never lost," he said. "Think for a moment if we could make GIS exactly that pervasive so our organizations would not be lost, our communities would not be lost, and our society would not be lost."

To illustrate how fast web GIS is maturing, Esri's Lauren Bennett demonstrated several new spatial analysis tools in ArcGIS Online. "We are able to answer common spatial questions using simple tools" Bennett said.

To see more videos from the conference, visit video.esri.com.

– Carla Wheeler, Esri Writer

LIDAR Community had the Event of the Year in Vienna!

RIEGL LIDAR 2013 User Conference, 25 - 27 June 2013, Vienna, Austria

With over 250 attendees from 40 countries, the RIEGL LIDAR 2013 International Airborne, Mobile, Terrestrial & Industrial User Conference turned out to be the LIDAR event of the year.

The conference took place at the Vienna Marriott, right in the magnificent historic city center of Vienna. Program highlights included presentations of the latest hardware and software by *RIEGL* and more than 80 User-, Partner-, and Scientific presentations by international leading LIDAR experts in various tracks. Special Sessions included presentations on bathymetry, architecture, geology, and UAV applications, to name just a few.

Moreover, 20 industry leading companies including Gold Sponsors Applanix, ESRI and Trimble exhibited and gave a partner presentation.

To kick off the conference, the new ***RIEGL* LMS-Q1560,** which represents the future of airborne laser scanning technology, was unveiled to the international audience. Only one day after the official unveiling, *RIEGL* gladly announced the first LMS-Q1560 sale to a long-standing customer in Canada.

RIEGL also presented several other exciting hardware and software news:

- the **VMS-250** single-scanner mobile mapper optimized for marine applications
- the **VMX-450-RAIL**: high end mobile mapping system optimized for usage on railways
- **RiSOLVE**, *RIEGL*'s new software package designed for use with the VZ-400 and VZ-1000 terrestrial laser scanners for collision investigation and scene reconstruction, simplifying the acquisition process and reducing processing time dramatically
- **RiPRECISION**, *RIEGL*'s new software package created for use with the *RIEGL* family of mobile scanning systems. The powerful software adjusts overlapping data to create a very precise point cloud for the end user.
- Right in time for the conference, technology startup rapidlasso has released an open data exchange format called "PulseWaves" for storing full waveform LiDAR data.

In addition to the conference itself, technical workshops were provided, a tour of the *RIEGL* headquarters in Horn was given and a technical excursion to *RIEGL's* airborne partners Airborne Technologies, Diamond Airborne Sensing and Schiebel in Wiener Neustadt south of Vienna was made.

The Highlight of the social program was Wednesday evening's Gala Dinner. The *RIEGL* community came together in a spectacular, ultra-modern ambience for high class entertainment in the heart of Vienna, and spent a wonderful evening together.

National cartography of Peru to be digitized

The National Geographic Institute (IGN), the mapping agency of Peru, has launched a project for digitisation of national cartography. The idea of the project is to have a high precision data in order to contribute to the growth of public and private investments that can benefit from this updated mapping information. The institute is looking at generating a basic cartography scale 1/25, 000 of Moquegua and Tacna Departments. *www.ign.gob.pe/*

Geo data online in a German State

Mecklenburg-Vorpommern, a federal state in north Germany is planning to implement "Municipal Geo-information System" in all its municipalities. The aim is to create an online portal to provide geodata collected through local government's GIS system. Currently, the local government has data on land-use plans, road cadastre, land registry tree etc. It can be seen with reference to population and economic indicators. Once the data is put online, it will open up the possibility of meeting the INSPIRE Directive and EU regulations for spatial information in the European Union.

Indonesia promotes use of GIS for economic development

The Ministry for Development of Disadvantaged Regions is working together with the Geospatial Information Agency (formerly known as BAKOSURTANAL); Indonesia to support the development of several key sectors and industries in some of the country's most disadvantaged areas. The agency will be providing its expertise to promote the use of geospatial information to pump prime sectors such as agriculture, mining, energy, marine, tourism and telecommunications. *www.futuregov.asia*

Mapping a healthy future for SA children

With nearly a quarter of South Australian children overweight or obese, SA Health, in partnership with the state's local governments tackling the issue by developing community awareness and education policies, programs partnerships and infrastructure. Key to this strategy is the Obesity Prevention and Lifestyle (OPAL) program, which supports children's health through educating their families and communities. Part of the OPAL program is an eight year evaluation which uses GIS technology to monitor and analyse existing infrastructure, environments and resources – such as playgrounds and recreation facilities – to better target state and local governments' policy and intervention efforts. *http://esriaustralia.com.au*

Poland to implement Geoportal 2

The Head Office of Geodesy and Cartography of Poland is getting ready to implement Geoportal 2. The main goal of the project is to provide citizens, businesses and public administration access to government registers, which contain high quality, current and reliable data. As a result of the project, services related to spatial data will also be enabled.

Atlas Qatar ranked first at Esri UC

Atlas Qatar and its digital publication were ranked first in the world during the International Conference of GIS, organized by the Esri in San Diego, USA. The Ministry of Development Planning & Statistics (MDPS) participated in this conference with its up-to-date publications, Atlas Qatar and Digital Atlas, which were developed and drafted using the latest techniques of GIS. *www.gulf-times.com*

Ghana is developing national spatial planning framework

Ghana is developing a National Spatial Development Framework to guide the provision of amenities and facilities in the various districts and regions in the country, said Mr Richard Geier, Manager of the Framework Programme, recently. He said the framework would facilitate a balanced redistribution of urban population, adding that, "it would enable development planners to know which districts are under-served and those that are over-served in terms of the development of infrastructure and distribution of amenities". He called for the enactment of legislation on land use spatial planning, to strengthen the legal framework for land use. *www.ghanaweb.com*

Johor to map out rural roads digitally

Johor will be the first state in Malaysia to map out over 5,000 kilometres of its rural road network digitally to update and improve their management. The project will be carried out by Infra Desa Johor Sdn Bhd (IDJSB), a state-owned company that is responsible for the maintenance of these roads, and Universiti Teknologi Malaysia (UTM). IDJSB shall use the expertise of the lecturers and students of UTM's Faculty of Geoinformation and Real Estate. *www.nst.com.my*

First GPU-Accelerated Platform for Geospatial Int Analysts launched

NVIDIA has launched the NVIDIA® GeoInt Accelerator™ to enable security analysts to find actionable insights quicker and more accurately than ever before from vast quantities of raw data, images and video. It provides defense and homeland security analysts with tools that enable faster processing of high-resolution satellite imagery, facial recognition in surveillance video, combat mission planning using GIS data, and object recognition in video collected by drones. *www.nvidia.com*

Federal Security Geospatial Portal launched in UAE

Major General Ahmed Nasser Al Raisi, Director General of Central Operations, launched the first edition of the Federal Security Geospatial Portal, the first-of-its-kind in the region in terms of its institutional characteristics and its comprehensiveness of implementation. The portal includes tens of police and digital maps that are designed and developed internally through idea exchange and efforts made by international experts in the fields of GIS. The portal's aim is to serve over 18 security and police entities, and police stations at the UAE level.

Falcon 9 rocket to deliver RADARSAT Constellation to Orbit

Space Exploration Technologies was awarded a launch reservation contract with MacDonald, Dettwiler and Associates Ltd. (MDA) to support the largest space program to date in Canada, carrying the three satellites to orbit that will make up the RADARSAT Constellation Mission (RCM) on a Falcon 9 rocket in 2018. RCM is a three satellite configuration and will support Canada's need for maritime surveillance, disaster management and ecosystem monitoring. *www.spacex.com*

Pakistan approves Remote Sensing programme

The Executive Committee of the National Economic Council, Pakistan approved the project of Pakistan Remote Sensing Satellite (PRSS) located in Sindh and Punjab with cost of Rs.19695.0 million. The project is part of National Satellite Development Programme for space technology and its application will be in Pakistan, institutional capacity building of SUPARCO and relevant organizations. *www.app.com.pk*

First national carbon map using satellite imagery, LiDAR

Researchers have mapped the above ground carbon density throughout the Republic Panama in high resolution. This is the first time when such mapping has been done for an entire country. Researchers integrated field data with satellite imagery and high-resolution airborne Light Detection and Ranging (LiDAR) data to map the vegetation and to quantify carbon stocks.

Researchers from Smithsonian Tropical Research Institute (STRI), McGill University and UC-Berkeley found Panama to be an ideal laboratory to develop and test a method for quantifying aboveground carbon because of its complex landscapes, with variable topography, and diverse ecosystems. They combined ground-based plot sampling, satellite imagery, and LiDAR measurements from the Carnegie Airborne Observatory to carry out the project. The new system, described in Carbon Balance and Management, will greatly boost conservation and efforts to mitigate climate change through carbon sequestration. *http://cao.ciw.edu/*

Satellite imagery has revealed that Saudi Arabia is targeting Israel and Iran

Saudi Arabia doesn't have formal ties with Israel and treats Iran as enemy too. The satellite pictures show a previously undisclosed surface-to-surface missile base in the middle of the Saudi desert, the Telegraph reported. Analysts say they saw in the images at least two launch pads — one pointing toward Tel Aviv and another toward Tehran. *www.washingtontimes.com*

UAE contract to Astrium and Thales

The United Arab Emirates Armed Forces on July 22 contracted with Astrium Satellites and Thales Alenia Space of France to provide the two-satellite Falcon Eye high-resolution optical reconnaissance system.

It includes the construction of two satellites weighing less than 1,500 kilograms each; their separate launches in late 2017 and early 2018.

Industry officials said that they would use the same satellite platform as the French government's two Pleiades satellites, which operate in 700-kilometer polar low Earth orbits.

Thales Alenia Space will be providing the Falcon Eye imaging payload, with Astrium Satellites building the platform. Both companies said their hardware would be upgraded versions of what they built for Pleiades.

The contract was signed in Abu Dhabi during a ceremony presided over by Sheikh Mohammed Bin Zayed Al Nahyan, the UAE crown prince, who is also head of the UAE armed forces; and by Jean-Yves Le Drian, the French defense minister. *www.spacenews.com*

How Mercedes-Benz R&D is using Google Glass

Mercedes-Benz Research & Development North America (MBRDNA) is working on a way to take advantage of the Google's newest GPS-equipped device: Google Glass. According to MBRDNA President and CEO Johann Jungwirth, the company's ultimate goal on the Google Glass project is a "seamless" door-to-door transition between pedestrian directions and in-car GPS. *www.bizjournals.com*

Castrol partners with TomTom

Castrol has partnered with TomTom to study the impact of "stop-start" driving patterns across the world. The study already shows that drivers can experience as many as 18,000 stop-starts every year. The pioneering study that Castrol is undertaking with TomTom will discover the number of stop-starts in different cities around the world, and TomTom will use its precise travel and traffic information to analyse driving behaviour across the entire road network, all over the world. *http://corporate.tomtom.com*

Location, usage patterns to save iPhone battery life

The U.S. Patent and Trademark Office has published an Apple patent application for an intuitive mobile device control system that automatically powers down certain components.

In its aptly named application, "Power management for electronic devices," Apple describes a system that detects a mobile device owner's usage patterns, estimates the required energy needed to run the phone between charges, and dynamically turns hardware off or closes running software to achieve maximum battery life. *http://appleinsider.com*

Pedestrian navigation solution in real-world setting by Movea

Movea has collaborated with the SNCF, France's national railway company, as well as SK planet, a wholly owned subsidiary of SK telecom, South Korea's largest

Galileo update

Encouraging Galileo GNSS and EGNOS Use in the Mediterranean Basin

A European-Union funded consortium invites companies and public agencies from North Africa and the Middle East to submit ideas for extending Galileo GNSS and EGNOS use in the region. Eligible ideas could be for a small pilot project or research study, a technical training plan, and/or a publication or article. The submission deadline is August 25, 2013.

The countries in the target area are Algeria, Egypt, Israel, Jordan, Lebanon, Libya, Morocco, Palestine, Syria, and Tunisia. *www.euromedtrasport.eu*

European Space Agency - Ground Station Endures Freak Weather

Engineers manning Galileo's South Pacific ground station on New Caledonia found themselves marooned by heavy rains and a flash flood—though the station carried on operating regardless. Torrential rains lashed this French-administered group of islands at the start of July. The Galileo ground station near the capital Nouméa was caught in the deluge. Part of a growing worldwide network, it incorporates a Galileo Sensor Station that monitors the quality of navigation signals and an Uplink Station to relay navigation corrections to the satellites for rebroadcast to users. *www.satnews.com*

Britain Now Sees Potential of PRS Signal aboard Galileo

The British government's skepticism about the value of the encrypted, jam-resistant signal on Galileo satellite constellation has given way to an embrace of the signal as a future revenue source for British industry, government and industry officials said.

The Public Regulated Service (PRS) signal onboard Galileo will be available to European Union (EU) governments that provide security guarantees to specially designated Galileo program managers. Several European governments have said they plan to equip their emergency response teams and civil security forces. Several, notably France, have said they intend to supply their militaries with PRS-equipped hardware even as they maintain their use of the future military, or M-code, signal on the U.S. GPS satellites.

The British government in the past has openly questioned PRS's value, and even suggested that it has no place as a military component in a project that is financed and managed by civilian authorities. Some of this opposition was concerned that anyone expressing interest in PRS would be forced to pay for it. This led several European defense ministries to soft-pedal their support for it. That has now changed. *www.spacenews.com*

Galileo GNSS service centre opened in Spain

The European GNSS Service Centre (GSC) was opened this month in Torrejón de Ardoz, Madrid, Spain, and will give information on the status of the Galileo constellation to application service providers and other users. This will help companies and organisations that are reliant on the constellation to ensure they can maintain the provision of any relevant products or services. *www.surveyequipment.com*

mobile network operator, to test its indoor navigation solution in the real world. In two separate demos, users successfully navigated through two busy train stations that serve thousands of commuters on a daily basis. Movea relied solely on the Samsung Galaxy Nexus phone's built-in sensors to effectively guide users from one location to another. *www.movea.com.*

Predict your location years into the future

A new piece of software claims to be able to predict your location years into the future - even if you don't know where you'll be. 'Far Out' is the result of statistical research that looks at GPS data, learns your typical movements and then extrapolates to decide on your likely future location. The result, according to the team behind it, systems that can make "highly accurate" predictions about where you'll be years down the line. *www.huffingtonpost.co.uk*

Esri and MapmyIndia business alliance

Esri has announced a strategic alliance with MapmyIndia. MapmyIndia will migrate its data production environment to the ArcGIS platform, allowing it to leverage Esri's high-end cartographic production tools and workflows to expand its range of products. The alliance will provide Indian application developers and end users with a high-performance, cost-effective platform for GIS and location-based services development. In addition Esri's cloud-based ArcGIS Online will help democratize GIS data access throughout India with its low-cost subscription plans. *www.mapmyindia.com*

Ruckus buys YFind, navigates its way into indoor-positioning market

Wi-Fi services provider Ruckus Wireless acquired privately held indoor-positioning company YFind Technologies. Ruckus said it intends to use YFind's location-based services (LBS) and analytical capabilities in combination with Ruckus' Smart Wi-Fi technology, "transforming Ruckus Smart Wi-Fi networks into location-intelligent infrastructures."

US critical infrastructure sectors at risk from GPS

The US Department of Homeland Security has released a summary report on its evaluation of the risks to US critical infrastructure from GPS disruptions. The report states, "US critical infrastructure sectors are increasingly at risk from a growing dependency on GPS for positioning, navigation, and timing (PNT) services. Such dependencies are not always apparent."The report further states, "Detecting, locating, and disabling sources of GPS disruption remain a challenge," adding, "Economic losses, lowered consumer confidence, and safety-of-life issues are possible consequences to sectors from extensive GPS disruptions. *www.GPS.gov*

IRNSS-1A, India's First Navigation Satellite successfully launched

ISRO's Polar Satellite Launch Vehicle, PSLV-C22, successfully launched IRNSS-1A, the first satellite in the Indian Regional Navigation Satellite System (IRNSS) on July 2, 2013) from Satish Dhawan Space Centre, Sriharikota, India. After a flight of 20 minutes 17 seconds, the IRNSS-1A Satellite, weighing 1425 kg, was injected to the intended elliptical orbit of 282.46 km X 20,625.37 km.

After injection, the solar panels of IRNSS-1A were deployed automatically. ISRO's Master Control Facility (at Hassan, Karnataka) assumed the control of the satellite. All Navigation and Ranging Payload In Orbit Tests (IOT) are completed and all operations are normal. *www.isro.gov.in*

Russia to launch two GLONASS satellites after Proton disaster

"We are planning to launch two satellites from the Plesetsk space center [in northern Russia] to replenish the GLONASS orbital grouping following the recent Proton-M accident," said Nikolai Testoyedov, the head of the Information Satellite Systems (ISS) company, which manufactures satellites for the GLONASS project.

The first GLONASS is scheduled for launch in the beginning of September, and the second at the end of October, according to Testoyedov.

Russia loses $200 million satellites

Russian rocket carrying three navigation satellites worth around $200 million crashed shortly after lift-off from the Russian-leased Baikonur launch facility in Kazakhstan after its engines suddenly switched off.

Russian Prime Minster Dmitry Medvedev, who has said that Russia has lost 10 satellites in seven failed launches in just over one year, ordered tighter controls put in place to avoid more embarrassing mishaps, his spokeswoman told Interfax. *http://uk.reuters.com*

Foreign airlines urged to use GPS at San Francisco

Federal aviation officials in US have advised all foreign airlines to use a GPS system instead of visual reckoning and cockpit instruments when landing at San Francisco International Airport in the wake of the deadly Asiana Airlines crash.

The FAA issued the recommendation involving main runways at the airport, saying in a statement that it took the action after noticing an increase in aborted landings at the airport by some foreign carriers flying visual approaches into the airport. *http://abcnews.go.com*

GPS flaw could let terrorists hijack ships, planes

Captain Andrew Schofield and Todd Humphreys, a GPS expert at the University of Texas, used a GPS flaw to take control of the sophisticated navigation system aboard an $80 million, 210-foot super-yacht in the Mediterranean Sea. The world's GPS system is vulnerable to hackers or terrorists who could use it to hijack ships -- even commercial airliners, according to a frightening new study that exposes a huge potential hole in national security.

Using a laptop, a small antenna and an electronic GPS "spoofer" built for $3,000, GPS expert Todd Humphreys and his team at the University of Texas took control of the sophisticated navigation system aboard an $80 million, 210-foot super-yacht in the Mediterranean Sea. *www.foxnews.com*

Precise GPS measurement finds 117 km difference in Indo-Nepal border

Precise measurement using GPS has found that Indo-Nepal border is 117 km longer than previously believed. The latest survey has estimated the Indo-Nepal border was closer to 1,868 km, 117 km more than the official length of 1,751 km. An official emphasized it was technology – and not a change in the location of border pillars that stretched the Indo-Nepal borders. Previously, surveyors used to walk along the border with metal chains measuring short lengths and then adding them up. This time the surveyors used GPS to measure angles and distances. *www.hindustantimes.com*

AAI starts training staff on GPS-based navigation system

Moving a step closer towards implementation of satellite-based navigation system, the Airports Authority of India (AAI) has started training its staff to familiarize them with GPS-Aided Geo Augmented Navigation system (GAGAN). AAI had organised a three-day workshop-cum-training session for about 40 senior, instructor level, officials at the Civil Aviation Training College at Allahabad. *www.thehindubusinessline.com*

GPS for safety of houseboats in Kerala, India

A GPS-based fleet safety management system will be introduced for houseboats, the mascot of Kerala Tourism. The system will track houseboats and ensure the safety and security of tourists while they cruise the backwaters.

Besides tracking and locating houseboats on a GIS map and timely emergency response, the route travelled by a houseboat can also be "geo-fenced" to receive alerts on any route violations. *www.thehindu.com*

Lawmakers oppose Roskosmos funding reduction and GLONASS system scrapping

Members of the State Duma demand from the government to prevent reduction of Roskosmos programs funding, since it may lead to a scrap to GLONASS system functioning and Vostochny booster side building.

According to the minutes of the Duma Committee on Industry, adopted after the meeting with Roskosmos head Vladimir Popovkin, the proposal is to reduce budget funding of the state space program of Russia in 2014 for 11.7 billion rubles, in 2015 - for 13.5 billion rubles and for 40 billion rubles in 2016. In addition to this, the federal space program of Russia for 2006-2015 /FSP-2015/ already lacks of 10.5 billion rubles funding, and this year there has been a 2.3 billion rubles additional reduction in R&D under this program. *http://indrus.in*

NovAtel News

New Antennas by Novatel

AG-STAR GNSS antenna is cost-effective L1 GPS+GLONASS receiver plus antenna system is housed in a single, low profile, rugged enclosure. It is ideal for manual guidance and auto steer installations. Its design interface maximizes flexibility with two NMEA 0183 compatible RS-232 serial ports and a NMEA2000 compatible CAN port. One PPS output, an event mark input and three daylight readable status LEDs are also provided.

The **SMART6** antenna integrates NovAtel's powerful OEM6® GNSS receiver engine with its high performance Pinwheel® antenna technology. Tracking L1 and L2 GPS + GLONASS signals, and E1 Galileo and BeiDou B1 ready, it delivers scalable performance, from single-frequency positioning to centimetre-level accuracy using dual-frequency RTK tracking.

OEM638™ GNSS receiver card and the ProPak6™ enclosure

NovAtel has added OEM638™ GNSS receiver card and the ProPak6™ enclosure to its OEM6 family of high precision positioning products. The most advanced card within NovAtel's OEM6 GNSS receiver family, the OEM638 tracks all existing and planned constellations including GPS, Beidou, GLONASS, Galileo and QZSS.

The ProPak6 is NovAtel's most sophisticated GNSS enclosure product, offering metre-level to centimetre-level positioning in an extremely rugged, water resistant IP67 housing. Standardized software and hardware connections, including multiple RS-232/RS-422 serial ports, CAN Bus, USB host and device, as well as Bluetooth®, Wi-Fi and optional cellular radio, speeds time to market and maximizes user capabilities.

HI▸TARGET

ZTS Series Total Station

ZTS-120/120R

- Intelligent Calibration, USB Port&Bluetooth Optional
- Reflectorless Distance Measurement, Range Up To 350M
- Integrated Optical, Mechanical and Electrical Precision Ranging System, Accuracy: 2mm±2ppm
- High Efficient Absolute Encoder Angle Measuring System, Accuracy: 2″

Simply Powerful


ZTS-120R


ZTS-120

CE

Hi-Target Surveying Instrument Co., Ltd

www.hi-target.com.cn
www.gnss-gps.com

ADD:10th Floor,Chuangxin Building,Tian'an Technology Zone, No.555, North of Panyu Road,Panyu District,511400, Guangzhou City,China Tel: +86-20-22883930 Fax: +86-20-22883900 E-mail:info@zhdgps.com

TI Asahi Co., Ltd. & Zoller + Froehlich GmbH Sign OEM Agreement

TI Asahi Co., Ltd. and Zoller + Froehlich GmbH have signed OEM agreement for exclusive distribution worldwide of PENTAX branded 3D scanners by TI Asahi Co., Ltd. Under the agreement, Zoller + Froehlich GmbH will OEM-supply PENTAX branded high-precision, state of art 3D and 2D scanners to TI Asahi Co., Ltd, and TI Asahi Co., Ltd. will distribute them through its well-established sales channels of their world's distributors together with software for specific application which will make 3D scanners incorporated in various solution oriented systems, serving the needs of a variety of industries which require highly accurate 3D and 2D scanned data. Products to be OEM-supplied are PENTAX S-3180V, S-3180, S-3080 3D scanners and S2100 2D scanner. *www.tiasahi.com*

RTCM Issues an Amendment of its Standard for differential Global Navigation Satellite Systems

The Radio Technical Commission for Maritime Services (RTCM) Special Committee 104 has just completed an amendment to RTCM 10403.2, the widely-used "Version 3" standard for Differential Global Navigation Satellite System Services (DGNSS). RTCM's standard supports very high accuracy navigation and positioning through a broadcast from a reference station to mobile receivers. Looking forward to the use of new satellite positioning systems from Europe and China, the amendment introduces an ephemeris message for the Galileo Open Service (F/NAV), and also a set of BeiDou messages in the new Multiple Signal Message (MSM) format. The amended standard is available from RTCM at its secure online publication store. *www.rtcm.org*

Rohde & Schwarz adds simulated satellite system to vector signal generator

A new option on the SMBV100A vector signal generator from Rohde & Schwarz is a GNSS simulator aimed at developers of satellite-based navigation instruments. The new SMBV-K101 option allows developers to test GNSS receivers for specific effects such as obscuration and multipath propagation. Buildings, tunnels and bridges as well as reflections from concrete and glass surfaces affect the GNSS signal, regardless of whether the receiver is stationary or in motion, and this option makes it easy to configure these kinds of scenarios.

If the GNSS receiver of a navigation instrument or smartphone is located inside a vehicle, testing must also take into account the obscuring effect of the vehicle's metal body. The R&S SMBV-K102 option can simulate this obscuration and, if required, also the additional antenna pattern. *www.rohde-schwarz.com*

Premium services for ArcGIS Online Users by DigitalGlobe and Esri

Esri ArcGIS Online users will now have access to DigitalGlobe's Premium Services. The new offering brings expanded geospatial products and solutions to select users of ArcGIS Online on a subscription basis. With this exciting partnership, DigitalGlobe's Global Basemap, FirstLook, and Multispectral Premium Services can now be seamlessly integrated into the workflow of ArcGIS users, allowing them to access the most current imagery and information available directly from the source! *www.digitalglobeblog.com*

New Inertial system to SBG Systems, Ekinox Series

With integrated Dual Antenna GPS + GLONASS receiver, the Ekinox-D is a ready-to-use Survey Grade inertial navigation system which provides consistent true heading (0.05°). It is a high performance inertial navigation system which embeds a Dual Antenna L1/L2 GNSS receiver to deliver more robust heading and position, while increasing satellite reception availability. GNSS data and inertial information are fused by an Extended Kalman Filter (EKF) to improve data integrity. *www.sbg-systems.com*

New FARO® CAM2® SmartInspect software

FARO Technologies, Inc.has announced the new FARO CAM2 SmartInspect measurement software. The new software is highly suited to take measurements without CAD data. In developing the software, the focus was on - Simple, Intuitive operation and A Short learning phase. This means that even users with minimal background knowledge of 3D measurement technology can achieve very good measuring results within a short period of time. *www.faroasia.com*

Lockheed Martin GPS III Satellite prototype

Lockheed Martin recently delivered a full-sized, functional prototype of the next-generation GPS satellite to Cape Canaveral Air Force Station to test facilities and pre-launch processes in advance of the arrival of the first GPS III flight satellite.

The GPS III Non-Flight Satellite Testbed (GNST) arrived at the Cape on July 19 to begin to dry run launch base space vehicle processing activities and other testing that future flight GPS III satellites will undergo. *www.lockheedmartin.com/gps*

Field-ready RF recorder captures wideband multi-GNSS signals

AVERNA RP-5300 RF Recorder is specifically adapted for all GNSS applications, including Galileo, GPS, GLONASS, and Compass. System has two 50-MHz wide channels that can be tuned on any frequencies from 330 MHz to 2500 MHz. *http://www.averna.com*

Cm level accuracy for Mobile GIS Applications by Septentrio

Septentrio has joined forces with Esri BeLux in Belgium and Luxembourg to offer a user friendly mobile solution that is accurate up to 1 centimeter. This mobile solution combines the use of Esri ArcGIS for Mobile with a highly accurate GNSS device called AsteRx-m™ GeoPod. The combination of Esri software and the AsteRx-m™ GeoPod

operates seamlessly using standard, open interfaces on any professional tablet. *www.septentrio.com/geopod*

New TruPulse Laser rangefinders by Laser Technology

Laser Technology, Inc. has released two new TruPulse laser rangefinders, the 200X and 200L. Both measure slope distances and degree of inclination allowing the unit to calculate horizontal and vertical distances, height and 2D missing line values. The new TruPulse 200L is designed for the cost-conscious professional while the new TruPulse 200X caters to those who require a much higher degree of accuracy and overall durability.

Integrated GIS, Mapping receiver by Topcon

Topcon Positioning Systems (TPS), HiPer SR for GIS is a compact, integrated GNSS receiver with sub-meter accuracy. Additional, scalable options are available via OAF (Options Authorization File) upgrades, delivering accuracy levels of sub-decimeter and centimeter without the need for additional hardware. It can be paired with a Topcon controller and eGIS software, or used with Topcon's eGPS utility software to use with a third-party device and application. *www.topconpositioning.com*

Intel to acquire ST-Ericsson GNSS portfolio

Assuming that its deal to acquire ST-Ericsson's GNSS business closes soon, Intel Corporation will find itself with expanded opportunities – and competitive set – in the mobile location marketplace.

ST-Ericsson's G1960 chip, built with 40-nanometer CMOS technology, provides GPS, GLONASS, Quasi-Zenith Satellite System (Japan's QZSS), satellite-based augmentation system (SBAS), and assisted-GNSS functionality. A nascent BeiDou capability is reportedly also in the connectivity unit's technology mix.

MARK YOUR CALENDAR

September 2013

JISDM 2013
9 - 11 September
The University of Nottingham, UK
www.nottingham.ac.uk/engineering/conference/jisdm/index.aspx

Multi-GNSS environment for sustainable development
9 - 13 September 2013
Hoi An, Vietnam
http://navis.hust.edu.vn

Geo-Empower Middle East Summit
16-18 September
Dubai, UAE
www.fleminggulf.com/All-Categories

ION GNSS 2013
16 – 20 September
Nashville, Tennessee, USA
www.ion.org

GDI APAC 2013: Geospatial Defence & Intelligence 2013
17-18 September
Singapore
www.geospatialdefenceasia.com

FOSS4G 2013
17 – 21 September
Nottingham, UK
http://2013.foss4g.org/geohack/

FIG: LADM 2013
24 – 25 September
Kuala Lumpur, Malaysia
www.isoladm.org

International Symposium & Exhibition on Geoinformation (ISG 2013)
24 - 25 September
Kuala Lumpur, Malaysia
www.voronoi.com/isg2013

October 2013

Intergeo 2013
8 – 10 October
Essen, Germany
http://www.intergeo.de/en/index.html

UN-GGIM
16-18 October
Chengdu, Sichuan Province, China
http://ggim.un.org/

34th Asian Conference on Remote Sensing
20 – 24 October 2013
Bali, Indonesia
www.acrs2013.com/

ISGNSS 2013
22-25 October
Istanbul, Turkey
http://mycoordinates.org/isgnss-2013/

UN GGIM AP
28 – 30 October
Tehran, Iran

November 2013

GSDI World Conference (GSDI14) and the AfricaGIS 2013 Conference
4 - 8 November
Addis Ababa, Ethiopia
www.gsdi.org/gsdiconf/gsdi14/

ICG-8: Eighth Meeting of the International Committee on GNSS
10 – 14 November
Dubai, United Arab Emirates
www.oosa.unvienna.org/oosa/en/SAP/gnss/icg.html

SPAR Europe/European Lidar Mapping Forum
11-13 November
Amsterdam, The Netherlands
www.sparpointgroup.com/Europe/

ISPRS: Serving Society with Geoinformatics
11 – 17 November
Antalya, Turkey
www.isprs2013-ssg.org

December 2013

ION Precise Time and Time Interval Meeting (PTTI)
2 – 5 December
Bellevue, WA, United States
www.ion.org

Fourth ESA Colloquium on Galileo
4 – 6 December
Prague, Czech Republic
www.congrexprojects.com/13c15/

6th European Workshop on GNSS Signals and Signals Processing
5- 6 December
Munich, Germany
http://ifen.bauv.unibw.de/gnss-signals-workshop/

January 2014

ION International Technical Meeting
27-29 January
San Diego, California, USA
www.ion.org

March 2014

Munich Satellite Navigation Summit 2014
25 – 27 March
Munich, Germany
www.munich-satellite-navigation-summit.org

April 2014

ENC-GNSS 2014
14 – 17 April
Rotterdam, The Netherlands
www.enc-gnss2014.com

June 2014

XXV FIG Congress
16 – 21 June
Kuala Lumpur, Malaysia
www.fig.net


Visit us at INTERGEO 2013 in Essen, Germany
October 08 - 10, 2013 • Booth #A3.070
S320™
GNSS Survey
Receiver Solution
Visit us at INTERGEO 2013 in Essen, Germany
October 08 - 10, 2013 • Booth #A3.070
Built
Surveyor
Tough
Includes:
XF2™ Data Collector
Carlson SurvCE Data Collection Software
Whether you are doing GIS, Construction, Mapping, Land or Marine Surveying,
Hemisphere GPS' (now Hemisphere GNSS) S320™
can be tailored to your exact requirements.
SMS RTK & Texting • GNSS Configurable • SureTrack™ Intelligence • GSM Auto Corrections • 10-Hours Hot Swappable Battery Life • Includes XF2™ Data Collector and Carlson SurvCE Data Collection Software
www.S320Surveyor.com • Precision@HemisphereGPS.com
You Tube
Hemisphere GPS®


MAKE EXACT POSITIONING A SIXTH SENSE
H
SPAN®. Your positioning superhero.
SPAN is the world's most reliable OEM GNSS/INS technology, with the ability to provide continuous position, velocity and attitude. So an unprecedented mission—like landing an unmanned helicopter on a moving marine vessel—no longer stands in the way of success. Imagine how this kind of sensory superpower will help you rule in your world. As always, we'll keep your identity secret. To find out more, visit novatel.com/span or call you know who.
NovAtel
Integrate success into your .